

AN AXIOMATIC FRAMEWORK FOR N-AGENT AD HOC TEAMWORK: FROM SHAPLEY AXIOMS TO LEARNING

000
001
002
003
004
005 **Anonymous authors**
006 Paper under double-blind review
007
008
009
010

ABSTRACT

011 Open multi-agent systems are increasingly relevant for modelling the emerging real-
012 world domains such as smart grids and swarm robotics. This paper addresses the
013 recently posed problem of n-agent ad hoc teamwork (NAHT), where only a subset
014 of agents is controllable. We propose an axiomatic game-theoretic framework for
015 the NAHT, **formulated via a cooperative game model which differentiates between**
016 **the learning objectives of NAHT and MARL**. Within this framework, the axiomatic
017 characterization of the Shapley value—Efficiency, Symmetry, and Linearity—is
018 reinterpreted as structural constraints on individual value functions. This yields a
019 principled design space: enforcing all axioms recovers the Shapley value, while
020 dropping Efficiency yields the Banzhaf index, leading to our Banzhaf Machine
021 variant. As concrete instantiations, we develop Shapley Machine and Banzhaf
022 Machine, which enforce different subsets of axioms during learning. Implemented
023 on IPPO and POAM, these algorithms provide stronger performance.
024

1 INTRODUCTION

027 Multi-agent systems (MAS) have become a prominent paradigm for modelling the emerging real-
028 world tasks such as smart grids (Wang et al., 2021), railway network management (Zhang et al.,
029 2024), and swarm robotics (Nayak et al., 2023; Li et al., 2024). Reinforcement learning (RL) (Sutton
030 & Barto, 2018), and in particular multi-agent reinforcement learning (MARL), has shown promise for
031 solving such problems. However, MARL struggles under real-world conditions involving openness
032 (where the number of uncontrolled agents can vary) and generalization (where teammate behaviours
033 are unknown). To address these challenges, Wang et al. (2025) recently introduced the n-agent ad
034 hoc teamwork (NAHT), which extends MARL to settings with varying and potentially unknown
035 teammates. This paper builds on that problem, aiming to establish a theoretical foundation and a
036 general algorithmic approach for the NAHT.

037 The initial practical solution to the NAHT, POAM (Wang et al., 2025), augments the IPPO algo-
038 rithm (De Witt et al., 2020) with an embedding vector that represents each agent’s belief about other
039 agents’ potential behaviours. Although POAM improves empirical performance, it has several key
040 limitations: (i) It is designed heuristically without rigorous theoretical grounding, which undermines
041 trustworthiness—a critical concern for multi-agent systems (Hammond et al., 2025). (ii) **The funda-**
042 **mental distinction between the learning objectives of NAHT and MARL has been overlooked when**
043 **designing algorithms.** (iii) **POAM employs TD(λ) (Sutton, 1988) to train its critics, but its relation**
044 **to the NAHT objective remains unclear, leaving no guarantee that the learned value functions are**
045 **aligned with what NAHT fundamentally aims to address.**

046 The Shapley value (Shapley, 1953) is a classic payoff distribution rule from cooperative game theory
047 that has been widely applied in MARL (Wang et al., 2020; Li et al., 2021; Han et al., 2022; Wang
048 et al., 2022; Li et al., 2023). **Previously, the Shapley value’s formula was used to shape rewards or**
049 **value functions under the assumption that all agent are controlled, an assumption that breaks down**
050 **in the NAHT setting.** To investigate whether the Shapley value’s axioms can provide a principled
051 **foundation for solving the NAHT**, we propose a new axiomatic framework for the NAHT based on a
052 **cooperative game structure proposed by Dubey (1975) that can well describe the learning objective**
053 **of the NAHT. Specifically**, we build on its axiomatic characterization (Efficiency, Symmetry, and
Linearity) to structure individual value functions, which lets us both recover the Shapley value (when
all axioms hold) and design new variants by selectively relaxing a particular axiom.

The main contributions of this paper are as follows: (1) We cast the NAHT problem as a state-specific cooperative game, making explicit how openness alters its learning objective compared with the standard MARL. (2) We extend the Shapley value’s three axioms—Efficiency, Symmetry, and Linearity—to the NAHT setting and transform them into structural constraints for designing reinforcement learning algorithms. Notably, the Linearity axiom corresponds to truncated TD(λ) prediction (Cichosz, 1994). Enforcing all axioms recovers the Shapley value, while relaxing particular axioms—such as dropping Efficiency—yields alternative payoff allocations like the Banzhaf index (Banzhaf III, 1964). (3) By instantiating these constraints in learning, we propose the Shapley Machine, a generic algorithm that can be built on both IPPO and POAM, referred to as SM-IPPO and SM-POAM. In addition, when the Efficiency axiom is removed, the framework yields the Banzhaf Machine, producing the corresponding implementations BM-IPPO and BM-POAM.

We evaluate the Shapley Machine and Banzhaf Machine on modified versions of MPE-PP and SMAC adapted to the NAHT setting (Wang et al., 2025). They consistently outperform the base algorithms, and our experiments show that relaxing the Efficiency axiom may even surpass enforcing the full Shapley axioms in agent type generalization. The related work and complete mathematical proofs are left to Appendices A and D, respectively.

2 BACKGROUND

2.1 N-AGENT AD HOC TEAMWORK

In this section, we describe a problem setting for open multi-agent systems, referred to as n-agent ad hoc teamwork (NAHT) (Wang et al., 2025). The main challenges of NAHT are as follows: (1) coordination with potentially unknown types of teammates (generalization), and (2) coping with a varying number of uncontrolled teammates (openness). A decentralized partially observable Markov decision process (Dec-POMDP) (Oliehoek et al., 2016) is considered to formalize the problem. There is a team of agents \mathcal{M} whose size is denoted as M , a state space \mathcal{S} , a joint action space $\mathcal{A} = \times_{i \in \mathcal{M}} \mathcal{A}_i$, a per-agent observation space \mathcal{O}_i , a transition function $P_T : \mathcal{S} \times \mathcal{A} \rightarrow \Delta(\mathcal{S})$, a common reward function $R_t : \mathcal{S} \times \mathcal{A} \rightarrow \mathbb{R}$, a discount factor $\gamma \in [0, 1]$ and an episode length $T \in \mathbb{Z}^+$. Each agent receives observations via an observation function $O_i : \mathcal{S} \times \mathcal{A} \rightarrow \Delta(\mathcal{O}_i)$. \mathcal{H}_i is defined as an agent i ’s space of observation and action histories. Each agent is equipped with a policy $\pi_i : \mathcal{H}_i \rightarrow \Delta(\mathcal{A}_i)$.

In this problem, there are two groups of agents: a set of controlled agents denoted as \mathcal{C} whose size is denoted as N , and a set of uncontrolled agents denoted as \mathcal{U} whose size is denoted as $M - N$. As NAHT is an open system, at the beginning of an multi-agent interaction process, a team of agents \mathcal{M} , consisting of N agents randomly drawn from the controlled agent pool \mathcal{C} and $M - N$ agents randomly drawn from the uncontrolled agent pool \mathcal{U} . For conciseness, each controlled agent is characterized by its policy, and the set of controlled agents can be expressed as $\mathcal{C}(\theta) = \{\pi_i^\theta\}_{i=1}^N$. The above sampling procedure is denoted as $X(\mathcal{U}, \mathcal{C}(\theta))$. The aim of NAHT is learning parameters θ to solve the following optimization problem:

$$\max_{\theta} \mathbb{E}_{\pi^{(\mathcal{M})} \sim X(\mathcal{U}, \mathcal{C}(\theta))} \left[\sum_{t=0}^T \gamma^t R_t \right], \quad (1)$$

where $\pi^{(\mathcal{M})}$ denotes the joint policy of a team of agents \mathcal{M} . Note that different number of controlled agents N would lead to various teams of agents \mathcal{M} .

2.2 REPRESENTATION OF COOPERATIVE GAMES AND THE SHAPLEY VALUE

Definition 2.1 (Representation of Cooperative Games (Dubey, 1975)). *We first define such a function that $v_C^z = z$, for any $z \in \mathbb{R}$. If $C \subseteq D$, $v_C^z(D) = z$, otherwise, $v_C^z(D) = 0$. For a cooperative game described by a characteristic function $v : 2^{\mathcal{M}} \rightarrow \mathbb{R}_{\geq 0}$, we can describe a set of such games over a team of agents \mathcal{M} by a set of basis games $\{v_C^1 \mid \emptyset \neq C \subseteq \mathcal{M}\}$, such as $\mathcal{G} = \{w \mid w = \sum k_C v_C^1, k_C \in \mathbb{R}, \emptyset \neq C \subseteq \mathcal{M}\}$. The analytic form of k_C is represented as: $k_C = \sum_{T \subseteq C} (-1)^{|C|-|T|} v(T)$.*

Representation of Cooperative Games. A cooperative game is usually described as a characteristic function $v : 2^{\mathcal{M}} \rightarrow \mathbb{R}_{\geq 0}$, where \mathcal{M} is a team of agents. An arbitrary cooperative game v can be

108 uniquely represented by a set of basis games $\{v_C^1 \mid \emptyset \neq C \subseteq \mathcal{M}\}$ (Dubey, 1975), as delineated in
 109 Definition 2.1. In this paper, we focus on investigating how cooperative games are approximated
 110 over a team of agents. **Therefore, we only consider function values $v(\mathcal{M})$ and $v_C^1(\mathcal{M})$ for a**
 111 **team of agents \mathcal{M} , instead of other coalitions $C \subset \mathcal{M}$.** As per previous work in MARL (Wang
 112 et al., 2020), we consider the superadditive games as the game class of \mathcal{G} , which is suitable for a
 113 cooperative multi-agent task such as NAHT (see Appendix B.2 for more details). More specifically,
 114 the condition for \mathcal{G} restricted to superadditive games is: $k_C \geq 0$.

115 **Theorem 2.2 (Axioms of Shapley Values** (Dubey, 1975)). *Shapley value is a unique payoff allocation*
 116 *function on the cooperative game space \mathcal{G} , satisfying Efficiency, Symmetry and Additivity.*

117 **Shapley Values.** The Shapley value $\phi : \mathcal{G} \rightarrow \mathbb{R}^M$ is a multidimensional linear transformation defined
 118 on the set of cooperative game \mathcal{G} , given that there are M agents in total. Each dimension of ϕ indicates
 119 the payoff allocation to an agent. It has been proved that Shapley value is a unique payoff allocation
 120 function on the set of cooperative games \mathcal{G} which satisfies the following axioms: Efficiency, Symmetry
 121 and Additivity (Dubey, 1975),¹ highlighted in Theorem 2.2. Efficiency and Symmetry have been well
 122 investigated in the literature of multi-agent reinforcement learning (Wang et al., 2020; Li et al., 2021;
 123 Han et al., 2021; Wang et al., 2022; Chai et al., 2024), but Additivity still lacks attention. In detail,
 124 Additivity means that $\phi(w_1 + w_2) = \phi(w_1) + \phi(w_2)$, for any cooperative games $w_1, w_2 \in \mathcal{G}$. If we
 125 consider m possible games, then we have the following expression: $\phi(\sum_{i=1}^m w_i) = \sum_{i=1}^m \phi(w_i)$,
 126 where $w_1, w_2, \dots, w_m \in \mathcal{G}$ and the sum $\sum_{i=1}^m w_i$ can be seen as a game’s value reproduced by the
 127 above games’ values. Linearity is a stronger condition than Additivity (Dubey, 1975; Young, 1985).
 128 Specifically, Linearity requires $\phi(\sum_{i=1}^m \alpha_i w_i) = \sum_{i=1}^m \alpha_i \phi(w_i)$, for $\alpha_i \in \mathbb{R}$. As a special case,
 129 setting all $\alpha_i = 1$ recovers Additivity. **In this paper, we focus on the Linearity axiom to establish**
 130 **Additivity, which underpins the derivation of our method.**

3 GAME-STRUCTURED N-AGENT AD HOC TEAMWORK

134 To fit the dynamic environment setting in NAHT, we extend the cooperative game space \mathcal{G} to the state
 135 space \mathcal{S} of Dec-POMDP, forming a set of state-specific cooperative games. In more detail, for each
 136 state $s \in \mathcal{S}$ we have a state-specific cooperative game space $\mathcal{G}(s) = \{w_s \mid w_s = \sum k_C v_{C,s}^1, k_C \in$
 137 $\mathbb{R}, \emptyset \neq C \subseteq \mathcal{M}\}$, which is generated by a set of basis games $\{v_{C,s}^1 \mid \emptyset \neq C \subseteq \mathcal{M}\}$.

138 **Remark 3.1.** *Given a fixed state $s \in \mathcal{S}$, $\mathcal{G}(s)$ is isomorphic to a real coordinate space \mathbb{R}^{2^M-1} ,*
 139 *consistent with the structure of \mathcal{G} . As a result, all properties for \mathcal{G} also hold for $\mathcal{G}(s)$.*

140 **Definition 3.2 (Game-Structured NAHT).** $\mathcal{G}_{\text{NAHT}} = \times_{s \in \mathcal{S}} \mathcal{G}(s)$ denotes the set of all NAHT
 141 processes, where each element is a tuple of state-specific cooperative game values, specifying a team
 142 of agents \mathcal{M} , a state space \mathcal{S} , and weightings k_C associated with basis games of all non-empty
 143 coalitions $\emptyset \neq C \subseteq \mathcal{M}$.

144 By aggregating the state-specific cooperative game spaces for possible states, we represent possible
 145 NAHT processes for a team of agents as a structure $\mathcal{G}_{\text{NAHT}}$, as described in Definition 3.2. The insight
 146 is as follows: (1) Each state-specific cooperative game value captures the characteristics of a team’s
 147 performance in an NAHT process initiated from the corresponding state; (2) The characteristics of
 148 state-specific cooperative game values are shaped following the principle of the cooperative game
 149 theory (see Definition 2.1) which reflects the contributing factor of every agent. Thus, ignoring any
 150 single agent would induce bias to game values; (3) A state-specific cooperative game value can be
 151 decomposed into two learning curricula, each aligned with a distinct learning sub-objective—learning
 152 **internal cooperation** among controlled agents and learning **external teamwork** with uncontrolled
 153 agents:

$$v_s = \underbrace{\sum_{C_{int} \in \mathcal{P}_+(\mathcal{C})} k_{C_{int}} v_{C_{int},s}^1}_{\text{Internal Cooperation}} + \underbrace{\sum_{C_{ext} \in \mathcal{P}_+(\mathcal{M}) \setminus \mathcal{P}_+(\mathcal{C})} k_{C_{ext}} v_{C_{ext},s}^1}_{\text{External Teamwork}}$$

158 where $\mathcal{P}_+(\cdot)$ indicates the powerset of a set excluding the empty set. Related to the NAHT, variation in
 159 the number of controlled agents requires learning to establish internal cooperation, whereas variation

160 ¹For an arbitrary characteristic function game value, Shapley value is uniquely determined by the Efficiency,
 161 Additivity, Symmetry, and Dummy Player axioms (Chalkiadakis et al., 2011)[Chap. 2]. Since the Dummy Player
 162 axiom is already embedded in the basis game value construction of Dubey (1975), it is automatically satisfied.

162 in the number and types of uncontrolled agents demands learning strategies for robust external
 163 teamwork. In contrast, the standard MARL only requires learning to establish internal cooperation
 164 among a fixed number of controlled agents with no consideration of any uncontrolled agent, so it
 165 does not necessarily require any complex structure for the learning curriculum.

166 **Remark 3.3.** A state-specific cooperative game space $\mathcal{G}(s)$ is isomorphic to \mathbb{R}^{2^M-1} . The N
 167 controlled agents \mathcal{C} is a subset of a team of agents \mathcal{M} , and the $M - N$ uncontrolled agents
 168 $\mathcal{U} := \mathcal{M} \setminus \mathcal{C}$ is necessary for evaluating the controlled agents' policies (see Eq. 1). The ignorance of
 169 uncontrolled agents will reduce the $\mathcal{G}(s)$ to a subspace $W := \mathbb{R}^{2^N-1}$, and the **external teamwork**
 170 will be totally neglected. This introduces bias, as interpreted by the inter-vector angle before and
 171 after ignoring uncontrolled agents, which is explained in Example 3.4.

172 **Example 3.4.** As shown in Figure 1, suppose we have a team of agents $\mathcal{M} = \{1, 2\}$ for a state s ,
 173 where $\mathcal{C} = \{1\}$ and $\mathcal{U} = \{2\}$. θ is the angle between two vectors representing two situations, such
 174 that $w_s \in W = \text{span}\{v_{\{1\},s}^1\}$ and $u_s \in \mathcal{G}(s) = \text{span}\{v_{\{1\},s}^1, v_{\{2\},s}^1, v_{\{1,2\},s}^1\}$. It is obvious that
 175 $w_s(\mathcal{M})$ as a projection of $u_s(\mathcal{M})$ loses information about the **external teamwork**.

177 4 FROM SHAPLEY AXIOMS TO LEARNING FOR NAHT

180 In the following subsections, we show how to incorporate Markovian
 181 dynamics and how to extend the Shapley value's axioms to the state-
 182 specific cooperative game space for the NAHT. Together, these com-
 183 ponents establish an **axiomatic framework** in which individual value
 184 functions are shaped by structural constraints derived from the axioms.
 185 This framework provides a principled design space: enforcing all ax-
 186 ioms yields Shapley values, while relaxing some leads to alternatives
 187 such as the Banzhaf index. Moreover, it shows a close connection
 188 between the Linearity axiom and $\text{TTD}(\lambda)$.

189 4.1 A PRELIMINARY RESULT

191 By Definition 2.1, we have the expression $v_{C,s}^z = zv_{C,s}^1$, for any $z \in$
 192 \mathbb{R} , such that the condition that if $C \subseteq D$, $v_{C,s}^z(D) = z$, otherwise,
 193 $v_{C,s}^z(D) = 0$, still holds.

194 **Lemma 4.1.** Given a fixed state $s \in \mathcal{S}$, each state-specific coop-
 195 erative game's value $v_s \in \mathcal{G}(s)$ can be uniquely represented by:
 196 $v_s = \sum_{\emptyset \neq C \subseteq \mathcal{M}} k'_C \cdot v_{C,s}^z$, where $k'_C = \frac{k_C}{z}$ and $z \neq 0$.

197 By Lemma 4.1, a cooperative game can be equivalently represented by
 198 the form: $v_s = \sum_{\emptyset \neq C \subseteq \mathcal{M}} k'_C \cdot v_{C,s}^{v_s(\mathcal{M})}$ with setting $z = v_s(\mathcal{M})$ and $k'_C = \frac{k_C}{v_s(\mathcal{M})}$, and $v_s(\mathcal{M}) \neq 0$.²
 199 Herein, the set of $v_{C,s}^{v_s(\mathcal{M})}$ become a set of new basis games and k'_C are their corresponding weightings.

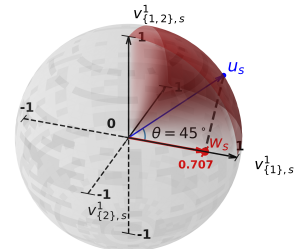
200 **Proposition 4.2.** For the class of superadditive games formed by a set of basis games $\{v_{C,s}^z | \emptyset \neq$
 201 $C \subseteq \mathcal{M}\}$, it holds that $k_C \geq 0$, for all $\emptyset \neq C \subseteq \mathcal{M}$.

202 Following discussion in Section 2.2, we aim to restrict the state-specific cooperative game class to
 203 the superadditive games. By Proposition 4.2, we can conclude that $k'_C \geq 0$ is a sufficient condition
 204 for v_s belonging to the superadditive game class. **In other words, $k'_C \geq 0$ is a key condition for**
 205 **reaching cooperation within a team of agents.**

206 Introducing a **linear multidimensional operator** $\phi : \mathcal{G}(s) \rightarrow \mathbb{R}^M$ on a state-specific cooperative
 207 game v_s defined by Lemma 4.1, we derive the following formula such that:

$$212 \phi(v_s) = \phi \left(\sum_{\emptyset \neq C \subseteq \mathcal{M}} k'_C \cdot v_{C,s}^{v_s(\mathcal{M})} \right), \quad (2)$$

213 ²If $v_s(\mathcal{M}) = 0$, it implies that a team of agents unable to cooperate, contradicting the purpose of the NAHT.



214 Figure 1: Example of state-
 215 specific cooperative games.
 216 The red and blue vectors
 217 are two games represented
 218 by different basis game
 219 sets, denoted by w_s and
 220 u_s . Their difference is
 221 measured by the θ . The
 222 shading area in red indicates
 223 the range of generated co-
 224 operative games with that
 225 $k_C \geq 0$ and $\sum(k_C)^2 = 1$.

216 where each $v_{C,s}^{v_s(\mathcal{M})}$ becomes a new basis game and k'_C is its corresponding new weighting. By the
 217 Linearity axiom of ϕ , we can transform Eq. 2 as follows:
 218

$$219 \quad 220 \quad 221 \quad \phi(v_s) = \sum_{\emptyset \neq C \subseteq \mathcal{M}} k'_C \cdot \phi(v_{C,s}^{v_s(\mathcal{M})}). \quad (3)$$

222 4.2 INCORPORATING MARKOVIAN DYNAMICS INTO GAME-STRUCTURED NAHT

224 For brevity, we rewrite $v_{C,s}^{v_s(\mathcal{M})}(\mathcal{M})$ as $V(C, s)$ for all $C \subseteq \mathcal{M}$. Then, we get the following fact:
 225

226 **Fact 4.3.** $V(C_1, s) = V(C_2, s) = \dots = V(\mathcal{M}, s) = v_s(\mathcal{M})$ for all $C_i \in \mathcal{P}_+(\mathcal{M})$, as per
 227 Definition 2.1 and $\mathcal{M} \supseteq C_i$, where $\mathcal{P}_+(\mathcal{M})$ indicates the powerset of \mathcal{M} excluding the empty set.

228 Continued from the game-structured NAHT defined in Section 3, we now introduce Markovian
 229 dynamics to establish connection between state-specific cooperative game values of consecutive
 230 states, adapting to the environmental condition in the Dec-POMDP (Oliehoek et al., 2016). The only
 231 postulate is that each state-specific cooperative game value can be represented in the form of rewards,
 232 such that $v_{s_t}(\mathcal{M}) = \mathbb{E}_\pi[\sum_{\tau=0}^{T-t-1} \gamma^\tau R_{t+\tau} \mid s_t] \in \mathcal{G}(s)$, following the notation in Section 2.1. By the
 233 convention of RL (Sutton & Barto, 2018)[Chap. 7], it is feasible to use the **n-step return** to express
 234 the $v_{s_t}(\mathcal{M})$ under a **fixed horizon** \bar{n} , such that:
 235

$$236 \quad 237 \quad v_{s_t}(\mathcal{M}) = \mathbb{E}_\pi \left[\sum_{\tau=0}^{\bar{n}-1} \gamma^\tau R_{t+\tau} + \gamma^{\bar{n}} v_{s_{t+\bar{n}}}(\mathcal{M}) \mid s_t \right] := \mathbb{E}_\pi [G_{t:t+\bar{n}} \mid s_t]. \quad (4)$$

238 **Definition 4.4 (Size-Lexicographic Coalition Order and Horizon Assignment).** Set $m := 2^M - 1$.
 239 Fix a size-lex enumeration (C_1, \dots, C_m) satisfying: (1) $|C_i| \leq |C_{i+1}|$ for all i (nondecreasing
 240 by size); (2) within each size, ties are broken by a fixed total order (e.g., lexicographic over agent
 241 indices). Define horizons by $n_1 := 1, n_i := n_{i-1} + 1$ ($i \geq 2$). Finally, set the basis game values as:
 242

$$243 \quad V(C_i, s) := \mathbb{E}_\pi[G_{t:t+n_i} \mid s_t = s], \quad (i = 1, \dots, m).$$

244 We justify Definition 4.4 in Appendix C by illustrating the alignment between the variance ordering
 245 of $V(C_i, s)$ and that of $\mathbb{E}_\pi[G_{t:t+n_i} \mid s_t = s]$.

246 **Proposition 4.5.** Under Definition 4.4, for every $s \in \mathcal{S}$,

$$247 \quad (V(C_1, s), \dots, V(C_m, s)) = (\mathbb{E}_\pi[G_{t:t+n_1} \mid s], \dots, \mathbb{E}_\pi[G_{t:t+n_m} \mid s]),$$

248 and, by Fact 4.3, each coordinate is cardinally equal to $V(\mathcal{M}, s)$.
 249

250 *Proof.* Immediate from the definition of $V(C_i, s)$; cardinal equality follows from Fact 4.3. \square

253 By Fact 4.3 and Proposition 4.5, we obtain the following formula that aligns basis game values of
 254 various coalitions to their n-step returns with corresponding horizons $1 \leq n \leq m$:

$$255 \quad 256 \quad 257 \quad V(C_n, s_t) = \mathbb{E}_\pi \left[\sum_{\tau=0}^{n-1} \gamma^\tau R_{t+\tau} + \gamma^n V(\mathcal{M}, s_{t+n}) \mid s_t \right], \forall \emptyset \neq C_n \subseteq C_{n+1}, C_m = \mathcal{M}. \quad (5)$$

259 4.3 LINEARITY AXIOM FOR GAME-STRUCTURED NAHT

261 Recall that $v_{C_n, s_t}^{v_{s_t}(\mathcal{M})}(\mathcal{M})$ is denoted by $V(C_n, s_t)$, and $v_{s_t}(\mathcal{M})$ is denoted by $V(\mathcal{M}, s_t)$. Substituting
 262 Eq. 5 into the Linearity axiom in Eq. 3, we obtain the following formula:
 263

$$264 \quad 265 \quad \phi(V(\mathcal{M}, s_t)) = \sum_{n=1}^m k'_{C_n} \cdot \mathbb{E}_\pi \left[\sum_{\tau=0}^{n-1} \gamma^\tau \phi(R_{t+\tau}) + \gamma^n \phi(V(\mathcal{M}, s_{t+n})) \mid s_t \right]. \quad (6)$$

266 By linearity of the expectation operator, we obtain that:
 267

$$268 \quad 269 \quad \phi(V(\mathcal{M}, s_t)) = \mathbb{E}_\pi \left[\sum_{n=1}^m k'_{C_n} \cdot \sum_{\tau=0}^{n-1} \gamma^\tau \phi(R_{t+\tau}) + \gamma^n \phi(V(\mathcal{M}, s_{t+n})) \mid s_t \right], \quad (7)$$

270 where the term within the $\mathbb{E}_\pi[\cdot]$ takes the form of **truncated λ -return** (Sutton & Barto, 2018)[Chap. 271 12], if all k'_{C_n} are seen as weightings for n-step return components.

273 In principle, we aim to learn $\phi_i(V(\mathcal{M}, s_t))$ directly for each controlled agent $i \in \mathcal{C}$. **For brevity, we**
274 **represent each $\phi_i(V(\mathcal{M}, s_t))$ as $V_i(s_t)$, and $\phi_i(R_t)$ as $R_{t,i}$, respectively.** By sampling trajectories using a joint policy π , we derive the following TD(λ) error $\delta_{t,i}$ (Sutton & Barto, 2018)[Chap. 275 12] for each agent i such that:

$$277 \quad \delta_{t,i} := \sum_{n=1}^m k'_{C_n} \cdot \sum_{\tau=0}^{n-1} (\gamma^\tau R_{t+\tau,i} + \gamma^n V_i(s_{t+n})) - V_i(s_t). \quad (8)$$

280 4.4 EFFICIENCY AXIOM FOR GAME-STRUCTURED NAHT

282 **Proposition 4.6 (Representation of Transformed Rewards).** *Given the condition $\sum_{i=1}^M \phi_i(R_t) =$
283 R_t , the payoff allocation defined on rewards R_t , can be expressed as:*

$$285 \quad \phi_i(R_t) := R_t - \sum_{j \neq i} (\phi_j(V(\mathcal{M}, s_t)) - \gamma \phi_j(V(\mathcal{M}, s_{t+1}))). \quad (9)$$

288 Note that $\phi(R_{t+\tau})$ in Eq. 7 has not yet been defined. For obeying the state-specific cooperative
289 game space $\mathcal{G}(s)$ for the multidimensional operator $\phi(\cdot)$, it is necessary to represent $\phi(R_{t+\tau})$ in
290 the form of $\phi(V(\mathcal{M}, s))$. To achieve this, we now introduce the Efficiency axiom to define $\phi(R_t)$.
291 To satisfy the Efficiency axiom such that $\sum_{i=1}^M \phi_i(V(\mathcal{M}, s_t)) = V(\mathcal{M}, s_t)$, it is reasonable to
292 presume its sufficient condition holds: $\sum_{i=1}^M \phi_i(R_t) = R_t$. Literally, each agent's value expansion
293 can be expressed independently with its own $\phi_i(R_t)$, which will be detailed in the next subsection.
294 Consequently, the resulting expression of $\phi_i(R_t)$ is presented in Proposition 4.6.

295 Substituting Eq. 9 into Eq. 8 with replacing $\phi_i(R_t)$ and $\phi_i(V(\mathcal{M}, s_t))$ by $R_{t,i}$ and $V_i(s_t)$, the $R_{t,i}$ in
296 Eq. 8 can be rewritten as follows:

$$298 \quad R_{t,i} = R_t - \sum_{j \neq i} (V_j(s_t) - \gamma V_j(s_{t+1})). \quad (10)$$

300 **Theorem 4.7 (Principle of Decomposing Value Functions** (Oliehoek et al., 2016)). *Given an
301 additively factored reward function, for any timestep t there is a factorization of the transition
302 function, such that the value of a finite-horizon factored Dec-POMDP is decomposable across agents.*

304 The condition $R_t = \sum_{i=1}^M R_{t,i}$ for deriving the Efficiency axiom is also referred to as additively
305 factored immediate reward function. Theorem 4.7 indicates that the Efficiency axiom always exists in
306 the Dec-POMDP, given a factorization scheme of the transition function in addition to an additively
307 factored immediate reward function. Recall that the NAHT is considered in the Dec-POMDP (see
308 Section 2.1). To guarantee the feasibility of the Efficiency axiom, another constraint is added to
309 implicitly facilitate searching for a factorization of the transition function such that:

$$310 \quad \sum_{i=1}^M V_i(s_t) = V(\mathcal{M}, s_t). \quad (11)$$

314 4.5 SYMMETRY AXIOM FOR GAME-STRUCTURED NAHT

315 **Theorem 4.8.** *The payoff allocation operator satisfying permutation-equivariance is a sufficient
316 condition for the Symmetry axiom.*

318 The Symmetry axiom means that two agents who contribute equally to every possible coalition
319 (excluding themselves) should receive equal payoff allocations (Chalkiadakis et al., 2011)[Chap.
320 2]. In the literature from Dubey (1975), it was described as the permutation-equivariance of an
321 multidimensional operator ϕ defined on the cooperative game value function, since **permutation-
322 equivariance is a sufficient condition for the Symmetry axiom** (see Theorem 4.8). As a result,
323 we will focus on how to construct such an operator fulfilling **permutation-equivariance**. Mathematically,
324 we can express this as: $\phi_{\sigma(i)}(v_s) = \phi_i(\sigma(v_s))$, where σ means relabelling agent IDs to

another ordering, e.g., from $(1, 2)$ to $(2, 1)$. Recall that in the settings of NAHT, the environment is defined as a Dec-POMDP, where the transition function is defined as $P_T(s_{t+1}|s_t, a_t)$ with a_t being a joint action set, implying that the environment is invariant to exchanging agent identities and the cooperative game values are identical under exchanging agent identities. For this reason, $v_s = \sigma(v_s)$ naturally holds. We now replace ϕ with V_i to keep consistency of notations as the above two axioms. The rest of requirement to make the permutation-equivariance hold is that the operator's output is changed consistently with permuting agent IDs, e.g., $(1, 2) \mapsto (2, 1) \Rightarrow (V_1, V_2) \mapsto (V_2, V_1)$. This implies that the operator's output of each agent ID should be invariant to permutation of its input, e.g., $V_i(\sigma(inp)) = V_i(inp)$.

Remark 4.9. *The structure of the operator for payoff allocations for fulfilling the Symmetry axiom is as follows: (1) The operator's output is changed consistently with permuting agent IDs. (2) The operator's output of each agent ID should be invariant to permutation of its input.*

4.6 FROM SHAPLEY AXIOMS TO LEARNING ALGORITHMS

Theorem 4.10. *Shapley Machine is an algorithm enforcing V_i to fulfil Efficiency, Symmetry and Linearity, so the V_i is the Shapley value for dynamic scenarios.*

The algorithm that enables individual values V_i to fulfil the Efficiency, Linearity and Symmetry axioms through learning is named **Shapley Machine**: (1) Shape individual rewards following Eq. 10 and set Eq. 11 as a regularization term, to fulfil the Efficiency axiom. (2) Implement the TD error following Eq. 8, to fulfil the Linearity axiom. The $k'_C > 0$ is implemented as geometric distribution following the convention of TD(λ) (Sutton & Barto, 2018)[Chap. 12]. (3) Structure the policy and value networks to fulfil the Symmetry axiom. Since the Linearity axiom is a sufficient condition for the Additivity axiom as mentioned in Section 2.2, the individual values V_i satisfying all those axioms in implementation realizes Shapley values for dynamic scenarios, as highlighted in Theorem 4.10. In implementation, we use two base algorithms satisfying the conditions of partial observations: POAM (Wang et al., 2025) and IPPO (De Witt et al., 2020) to realize Shapley Machine, referred to as: **SM-POAM** and **SM-IPPO**, respectively. The details of implementation are left to Appendix E.1.

Remark 4.11. *Banzhaf Machine is an algorithm generating V_i , fulfilling Symmetry and Linearity.*

Following the same principle of designing algorithms via axiomatic characterization, we also propose a variant that enforces the Linearity and Symmetry axioms while omitting Efficiency. Since the resulting V_i aligns with the Banzhaf index (Banzhaf III, 1964)³, we refer to this algorithm as the **Banzhaf Machine**. Analogous to the Shapley Machine implementations above, its instantiations on POAM and IPPO are denoted as **BM-POAM** and **BM-IPPO**, respectively.

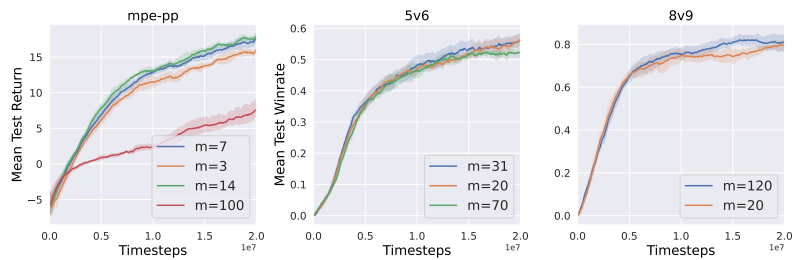
5 EXPERIMENTS

In experiments, we evaluate the proposed SM-POAM, SM-IPPO, BM-POAM and BM-IPPO on **the modified MPE-PP and SMAC tasks tailored to the NAHT settings** (Wang et al., 2025), against the counterpart baseline algorithms POAM and IPPO. The uncontrolled agents are taken from five pre-trained policies, which were trained in fully controllable MARL settings using the algorithms IPPO, MAPPO, VDN, QMIX, and IQL. To avoid confusion between the standard IPPO algorithm (trained under fully controllable MARL settings) and the version trained within the NAHT process (where only a subset of agents is controllable), we refer to the latter as IPPO-NAHT. Also, we validate the game-structured NAHT, a core concept in our theory, by setting the number of n-step return components considered in TTD(λ) using the number of basis games m . Since the number of basis games is far more than the preset episode length (511 vs. 150) in 10v11, we approximate the number of basis games to the episode length as a trade-off. About the 8v9 scenario, the number of basis games needed in theory is close to the episode length (127 vs. 120), so the number of basis games can be naturally approximated by the episode length. As a result, **for 8v9 and 10v11 Banzhaf Machine is equivalent to the baseline counterparts in implementation**. The details of baselines, experimental settings and evaluation metrics are provided in Appendix E. All results are obtained by first computing each metric with 128 episodes and then averaging these per-seed metrics across 5 random seeds, with 95% confidence intervals reported.

³Banzhaf index is a payoff allocation that satisfies Symmetry and Linearity (Additivity), but not vice versa.

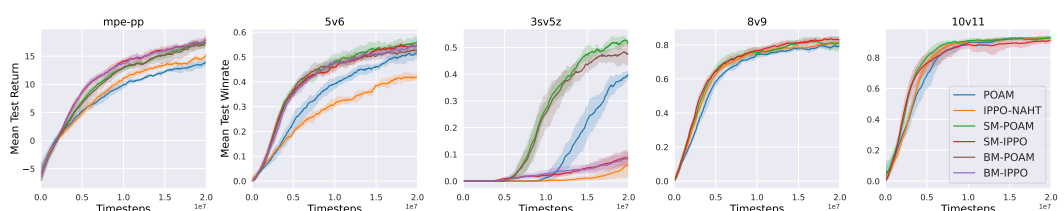
378 **Research Questions.** We focus on the following research questions in experimentation: (1) Is the
 379 number of coalitions m used to construct $\text{TTD}(\lambda)$ as defined in Proposition 4.5 a critical factor for
 380 learning performance? Answering this question provides empirical support for the rationality of our
 381 theoretical framework. (2) Are all the axioms characterizing the Shapley value equally appropriate
 382 across scenarios? This question highlights the flexibility of our axiomatic framework: rather than
 383 relying directly on the explicit Shapley formula as in prior work, we treat its axioms as design
 384 elements that can be selectively enforced or relaxed depending on the task. (3) Which axiom is
 385 key to generalization to unseen conventions or unseen agent types? The answer can emphasize the
 386 practicability of our axiomatic perspective.

387 5.1 MAIN RESULTS AND ANALYSIS



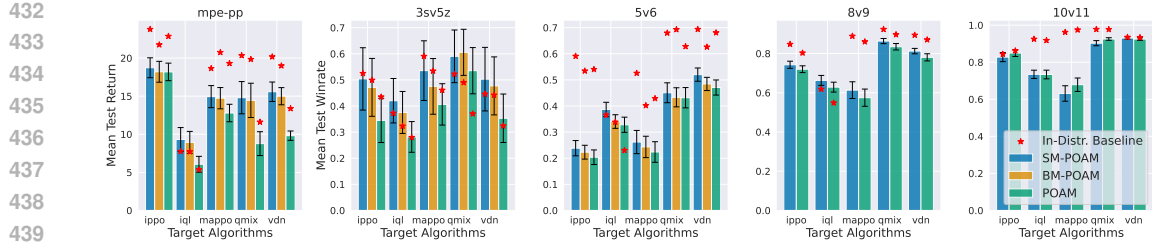
398 Figure 2: Experiments verifying that the number of n -step return components in $\text{TTD}(\lambda)$ can be
 399 determined by the number of non-empty basis games. In MPE-PP the number of basis games is
 400 $m = 7$, in 5v6 it is $m = 31$, and in 8v9 it is $m = 120$.

402 **Answer to Question 1.** We conduct experiments with varying numbers of basis games m using SM-
 403 POAM as the candidate algorithm. As shown in Figure 2, learning performance in MPE-PP and 8v9
 404 is sensitive to the choice of m , while in 5v6 it is comparatively robust. Overall, these results indicate
 405 that **setting the number of n -step return components as the number of non-empty basis games**
 406 **can nearly maximize learning performance**, thereby providing an empirical evidence to support
 407 the mathematical rationale behind Proposition 4.5. Although alternative theories or frameworks may
 408 exist for different choices of m —as seen in the good performance of MPE-PP and 5v6—**this does**
 409 **not undermine the validity of Proposition 4.5**.

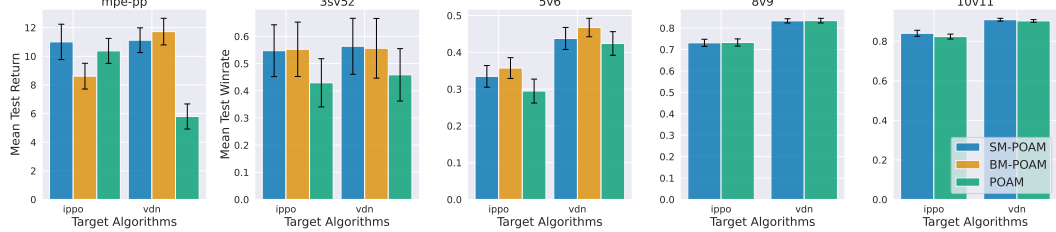


418 Figure 3: Evaluation curves during training in NAHT.

419 **Answer to Question 2.** We evaluate all baselines alongside our proposed algorithms. For the large-
 420 scale tasks 8v9 and 10v11, the base algorithms IPPO-NAHT and POAM are effectively equivalent to
 421 BM-IPPO and BM-POAM under the approximation of m , due to limited episode lengths, and are
 422 therefore omitted as separate implementations. Figure 3 shows that, for either IPPO-NAHT or POAM,
 423 at least one of their Shapley Machine or Banzhaf Machine variants achieves the best performance.
 424 Recall that Banzhaf Machine corresponds to dropping the Efficiency axiom. In MPE-PP and 3sv5z
 425 with IPPO-NAHT as the base, Banzhaf Machine performs on par with Shapley Machine. In most
 426 other scenarios (except 10v11 with IPPO-NAHT), Shapley Machine outperforms Banzhaf Machine,
 427 although sometimes by a narrow margin. Moreover, comparisons between the base algorithms and
 428 their Banzhaf counterparts in MPE-PP, 5v6, and 3sv5z underscore the importance of the Linearity
 429 axiom. Overall, the results suggest that **all three Shapley axioms generally enhance learning**
 430 **performance (in possibly unseen team compositions), but the Efficiency axiom can, in some**
 431 **cases, reduce it.** This confirms the value of our proposed axiomatic framework, which flexibly
 accommodates both Shapley- and Banzhaf-style formulations.



(a) Evaluation on unseen conventions (identical algorithms with different random seeds). The star denotes the in-convention baseline, and the histograms show performance on unseen conventions with error bars.



(b) Evaluation on unseen agent types. Train set: MAPPO, QMIX, IQL; test set: IPPO, VDN.

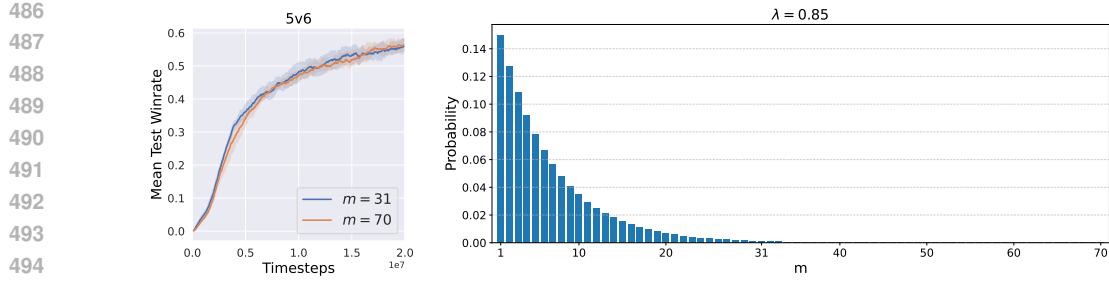
Figure 4: Out-of-distribution (OOD) evaluation after training, assessing unseen conventions and unseen agent types during training, between learned agents (POAM, SM-POAM and BM-POAM) and uncontrolled agent types (IPPO, VDN, IQL, QMIX and MAPPO). The performance is evaluated by averaging all pairings of N controlled and $M - N$ uncontrolled agents and their corresponding random seeds, called M–N score (Wang et al., 2025).

Answer to Question 3. We evaluate all baselines alongside our proposed algorithms after training, to test their capability of generalization to unseen conventions and unseen agent types, respectively. The evaluation is conducted by the best model saved during training for each random seed of running experiments. It can be seen from Figure 4a that SM-POAM outperforms both BM-POAM and POAM on all scenarios, except for the 10v11 due to the weak learning performance. This implies that **in general all Shapley axioms may be instrumental in tackling unseen conventions**. As seen from Figure 4b, the performance of BM-POAM is comparable to and even better than SM-POAM in most cases. This implies that **the Efficiency axiom could weaken the capability of generalization to unseen agent types**. This phenomenon recurs, and becomes even more pronounced, in the evaluation of IPPO-NAHT related algorithms, as shown in Figure 10b in Appendix F.3.

5.2 NUMBER AND WEIGHTINGS OF BASIS GAME VALUES

The weightings of basis game values (k'_C in Eq. 8) are set up by the probability values of a geometric distribution governed by λ in this paper, respecting the convention of RL. The λ will influence the shape of the geometric distribution. When the λ grows larger, the geometric distribution tends to be a longer tail with the probability decays slowly as the number of basis games m increases, and vice versa. In other words, **controlling m can be implemented by simply changing the weightings of basis game values, or equivalently, the λ , under the assumption of the geometric distribution**. To verify this result holding in the NAHT, we conduct a case study, as shown in Figure 5. It can be observed that the number of effective basis games (the probability values over which are non-zero) for $m = 31$ and $m = 70$ is the same under $\lambda = 0.85$, resulting in nearly identical learning performance. **This aligns with the conventional view of λ 's impact on $TTD(\lambda)$ in RL, primarily as a mechanism for controlling the tail length of the return (Sutton & Barto, 2018)[Chap. 12.3].**

Moreover, we demonstrate that even with the same number of basis games, the values of their corresponding weightings significantly influence the learning performance. As shown in Figure 6, given the same number of active basis games as $m = 7$, the learning processes with $\lambda = 0.5$ and $\lambda = 0.85$ result in diverse performance. **This provides an alternative insight into how λ influences $TTD(\lambda)$, diverging from the traditional RL perspective.**



486
487
488
489
490
491
492
493
494
495
496
497
498 (a) SM-POAM: $m = 31$ vs. (b) Demonstration of the shape of weightings of basis game values with
499 $m = 70$ for $\lambda = 0.85$. $\lambda = 0.85$.
500
501
502
503
504
505
506
507
508
509
510
511
512
513
514
515
516
517
518
519
520
521
522
523
524
525
526
527
528
529
530
531
532
533
534
535
536
537
538
539
540
541
542
543
544
545
546
547
548
549
550
551
552
553
554
555
556
557
558
559
560
561
562
563
564
565
566
567
568
569
570
571
572
573
574
575
576
577
578
579
580
581
582
583
584
585
586
587
588
589
590
591
592
593
594
595
596
597
598
599
600
601
602
603
604
605
606
607
608
609
610
611
612
613
614
615
616
617
618
619
620
621
622
623
624
625
626
627
628
629
630
631
632
633
634
635
636
637
638
639
640
641
642
643
644
645
646
647
648
649
650
651
652
653
654
655
656
657
658
659
660
661
662
663
664
665
666
667
668
669
670
671
672
673
674
675
676
677
678
679
680
681
682
683
684
685
686
687
688
689
690
691
692
693
694
695
696
697
698
699
700
701
702
703
704
705
706
707
708
709
710
711
712
713
714
715
716
717
718
719
720
721
722
723
724
725
726
727
728
729
730
731
732
733
734
735
736
737
738
739
740
741
742
743
744
745
746
747
748
749
750
751
752
753
754
755
756
757
758
759
759
760
761
762
763
764
765
766
767
768
769
770
771
772
773
774
775
776
777
778
779
779
780
781
782
783
784
785
786
787
788
789
789
790
791
792
793
794
795
796
797
798
799
800
801
802
803
804
805
806
807
808
809
809
810
811
812
813
814
815
816
817
818
819
819
820
821
822
823
824
825
826
827
828
829
829
830
831
832
833
834
835
836
837
838
839
839
840
841
842
843
844
845
846
847
848
849
849
850
851
852
853
854
855
856
857
858
859
859
860
861
862
863
864
865
866
867
868
869
869
870
871
872
873
874
875
876
877
878
879
879
880
881
882
883
884
885
886
887
888
889
889
890
891
892
893
894
895
896
897
898
899
900
901
902
903
904
905
906
907
908
909
909
910
911
912
913
914
915
916
917
918
919
919
920
921
922
923
924
925
926
927
928
929
929
930
931
932
933
934
935
936
937
938
939
939
940
941
942
943
944
945
946
947
948
949
950
951
952
953
954
955
956
957
958
959
959
960
961
962
963
964
965
966
967
968
969
969
970
971
972
973
974
975
976
977
978
979
979
980
981
982
983
984
985
986
987
988
989
989
990
991
992
993
994
995
996
997
998
999
1000
1001
1002
1003
1004
1005
1006
1007
1008
1009
1009
1010
1011
1012
1013
1014
1015
1016
1017
1018
1019
1019
1020
1021
1022
1023
1024
1025
1026
1027
1028
1029
1029
1030
1031
1032
1033
1034
1035
1036
1037
1038
1039
1039
1040
1041
1042
1043
1044
1045
1046
1047
1048
1049
1049
1050
1051
1052
1053
1054
1055
1056
1057
1058
1059
1059
1060
1061
1062
1063
1064
1065
1066
1067
1068
1069
1069
1070
1071
1072
1073
1074
1075
1076
1077
1078
1079
1079
1080
1081
1082
1083
1084
1085
1086
1087
1088
1089
1089
1090
1091
1092
1093
1094
1095
1096
1097
1098
1099
1099
1100
1101
1102
1103
1104
1105
1106
1107
1108
1109
1109
1110
1111
1112
1113
1114
1115
1116
1117
1118
1119
1119
1120
1121
1122
1123
1124
1125
1126
1127
1128
1129
1129
1130
1131
1132
1133
1134
1135
1136
1137
1138
1139
1139
1140
1141
1142
1143
1144
1145
1146
1147
1148
1149
1149
1150
1151
1152
1153
1154
1155
1156
1157
1158
1159
1159
1160
1161
1162
1163
1164
1165
1166
1167
1168
1169
1169
1170
1171
1172
1173
1174
1175
1176
1177
1178
1179
1179
1180
1181
1182
1183
1184
1185
1186
1187
1188
1189
1189
1190
1191
1192
1193
1194
1195
1196
1197
1198
1199
1199
1200
1201
1202
1203
1204
1205
1206
1207
1208
1209
1209
1210
1211
1212
1213
1214
1215
1216
1217
1218
1219
1219
1220
1221
1222
1223
1224
1225
1226
1227
1228
1229
1229
1230
1231
1232
1233
1234
1235
1236
1237
1238
1239
1239
1240
1241
1242
1243
1244
1245
1246
1247
1248
1249
1249
1250
1251
1252
1253
1254
1255
1256
1257
1258
1259
1259
1260
1261
1262
1263
1264
1265
1266
1267
1268
1269
1269
1270
1271
1272
1273
1274
1275
1276
1277
1278
1279
1279
1280
1281
1282
1283
1284
1285
1286
1287
1288
1289
1289
1290
1291
1292
1293
1294
1295
1296
1297
1298
1299
1299
1300
1301
1302
1303
1304
1305
1306
1307
1308
1309
1309
1310
1311
1312
1313
1314
1315
1316
1317
1318
1319
1319
1320
1321
1322
1323
1324
1325
1326
1327
1328
1329
1329
1330
1331
1332
1333
1334
1335
1336
1337
1338
1339
1339
1340
1341
1342
1343
1344
1345
1346
1347
1348
1349
1349
1350
1351
1352
1353
1354
1355
1356
1357
1358
1359
1359
1360
1361
1362
1363
1364
1365
1366
1367
1368
1369
1369
1370
1371
1372
1373
1374
1375
1376
1377
1378
1379
1379
1380
1381
1382
1383
1384
1385
1386
1387
1388
1389
1389
1390
1391
1392
1393
1394
1395
1396
1397
1398
1399
1399
1400
1401
1402
1403
1404
1405
1406
1407
1408
1409
1409
1410
1411
1412
1413
1414
1415
1416
1417
1418
1419
1419
1420
1421
1422
1423
1424
1425
1426
1427
1428
1429
1429
1430
1431
1432
1433
1434
1435
1436
1437
1438
1439
1439
1440
1441
1442
1443
1444
1445
1446
1447
1448
1449
1449
1450
1451
1452
1453
1454
1455
1456
1457
1458
1459
1459
1460
1461
1462
1463
1464
1465
1466
1467
1468
1469
1469
1470
1471
1472
1473
1474
1475
1476
1477
1478
1479
1479
1480
1481
1482
1483
1484
1485
1486
1487
1488
1489
1489
1490
1491
1492
1493
1494
1495
1496
1497
1498
1499
1499
1500
1501
1502
1503
1504
1505
1506
1507
1508
1509
1509
1510
1511
1512
1513
1514
1515
1516
1517
1518
1519
1519
1520
1521
1522
1523
1524
1525
1526
1527
1528
1529
1529
1530
1531
1532
1533
1534
1535
1536
1537
1538
1539
1539
1540
1541
1542
1543
1544
1545
1546
1547
1548
1549
1549
1550
1551
1552
1553
1554
1555
1556
1557
1558
1559
1559
1560
1561
1562
1563
1564
1565
1566
1567
1568
1569
1569
1570
1571
1572
1573
1574
1575
1576
1577
1578
1579
1579
1580
1581
1582
1583
1584
1585
1586
1587
1588
1589
1589
1590
1591
1592
1593
1594
1595
1596
1597
1598
1599
1599
1600
1601
1602
1603
1604
1605
1606
1607
1608
1609
1609
1610
1611
1612
1613
1614
1615
1616
1617
1618
1619
1619
1620
1621
1622
1623
1624
1625
1626
1627
1628
1629
1629
1630
1631
1632
1633
1634
1635
1636
1637
1638
1639
1639
1640
1641
1642
1643
1644
1645
1646
1647
1648
1649
1649
1650
1651
1652
1653
1654
1655
1656
1657
1658
1659
1659
1660
1661
1662
1663
1664
1665
1666
1667
1668
1669
1669
1670
1671
1672
1673
1674
1675
1676
1677
1678
1679
1679
1680
1681
1682
1683
1684
1685
1686
1687
1688
1689
1689
1690
1691
1692
1693
1694
1695
1696
1697
1698
1699
1699
1700
1701
1702
1703
1704
1705
1706
1707
1708
1709
1709
1710
1711
1712
1713
1714
1715
1716
1717
1718
1719
1719
1720
1721
1722
1723
1724
1725
1726
1727
1728
1729
1729
1730
1731
1732
1733
1734
1735
1736
1737
1738
1739
1739
1740
1741
1742
1743
1744
1745
1746
1747
1748
1749
1749
1750
1751
1752
1753
1754
1755
1756
1757
1758
1759
1759
1760
1761
1762
1763
1764
1765
1766
1767
1768
1769
1769
1770
1771
1772
1773
1774
1775
1776
1777
1778
1779
1779
1780
1781
1782
1783
1784
1785
1786
1787
1788
1789
1789
1790
1791
1792
1793
1794
1795
1796
1797
1798
1799
1799
1800
1801
1802
1803
1804
1805
1806
1807
1808
1809
1809
1810
1811
1812
1813
1814
1815
1816
1817
1818
1819
1819
1820
1821
1822
1823
1824
1825
1826
1827
1828
1829
1829
1830
1831
1832
1833
1834
1835
1836
1837
1838
1839
1839
1840
1841
1842
1843
1844
1845
1846
1847
1848
1849
1849
1850
1851
1852
1853
1854
1855
1856
1857
1858
1859
1859
1860
1861
1862
1863
1864
1865
1866
1867
1868
1869
1869
1870
1871
1872
1873
1874
1875
1876
1877
1878
1879
1879
1880
1881
1882
1883
1884
1885
1886
1887
1888
1889
1889
1890
1891
1892
1893
1894
1895
1896
1897
1898
1899
1899
1900
1901
1902
1903
1904
1905
1906
1907
1908
1909
1909
1910
1911
1912
1913
1914
1915
1916
1917
1918
1919
1919
1920
1921
1922
1923
1924
1925
1926
1927
1928
1929
1929
1930
1931
1932
1933
1934
1935
1936
1937
1938
1939
1939
1940
1941
1942
1943
1944
1945
1946
1947
1948
1949
1949
1950
1951
1952
1953
1954
1955
1956
1957
1958
1959
1959
1960
1961
1962
1963
1964
1965
1966
1967
1968
1969
1969
1970
1971
1972
1973
1974
1975
1976
1977
1978
1979
1979
1980
1981
1982
1983
1984
1985
1986
1987
1988
1989
1989
1990
1991
1992
1993
1994
1995
1996
1997
1998
1999
1999
2000
2001
2002
2003
2004
2005
2006
2007
2008
2009
2009
2010
2011
2012
2013
2014
2015
2016
2017
2018
2019
2019
2020
2021
2022
2023
2024
2025
2026
2027
2028
2029
2029
2030
2031
2032
2033
2034
2035
2036
2037
2038
2039
2039
2040
2041
2042
2043
2044
2045
2046
2047
2048
2049
2049
2050
2051
2052
2053
2054
2055
2056
2057
2058
2059
2059
2060
2061
2062
2063
2064
2065
2066
2067
2068
2069
2069
2070
2071
2072
2073
2074
2075
2076
2077
2078
2079
2079
2080
2081
2082
2083
2084
2085
2086
2087
2088
2089
2089
2090
2091
2092
2093
2094
2095
2096
2097
2098
2098
2099
2099
2100
2101
2102
2103
2104
2105
2106
2107
2108
2109
2109
2110
2111
2112
2113
2114
2115
2116
2117
2118
2119
2119
2120
2121
2122
2123
2124
2125
2126
2127
2128
2129
2129
2130
2131
2132
2133
2134
2135
2136
2137
2138
2139
2139
2140
2141
2142
2143
2144
2145
2146
2147
2148
2149
2149
2150
2151
2152
2153
2154
2155
2156
2157
2158
2159
2159
2160
2161
2162
2163
2164
2165
2166
2167
2168
2169
2169
2170
2171
2172
2173
2174
2175
2176
2177
2178
2179
2179
2180
2181
2182
2183
2184
2185
2186
2187
2188
2189
2189
2190
2191
2192
2193
2194
2195
2196
2197
2198
2198
2199
2199
2200
2201
2202
2203
2204
2205
2206
2207
2208
2209
2209
2210
2211
2212
2213
2214
2215
2216
2217
2218
2219
2219
2220
2221
2222
2223
2224
2225
2226
2227
2228
2229
2229
2230
2231
2232
2233
2234
2235
2236
2237
2238
2239
2239
2240
2241
2242
2243
2244
2245
2246
2247
2248
2249
2249<br

540 REPRODUCIBILITY STATEMENT
541

542 This paper is mixed of theoretical and algorithm contributions. To let the readers understand our main
543 contributions better, we present extra background knowledge in Appendix B. For all mathematical
544 claims in the paper, their justifications and proofs can be found in Appendices C and D. The
545 implementation details of our algorithms and baselines are shown in Appendix E.1. The metrics
546 for evaluating results, experimental settings and hyperparameters used in experiments are shown
547 in Appendices E.3, E.4 and E.5, respectively. The computational resources usage and the time for
548 experiments are exposed in Appendix E.6. Finally, we have uploaded an anonymous version of codes
549 to supplementary materials.

550
551 THE USE OF LARGE LANGUAGE MODELS
552

553 We made limited use of large language models (LLMs) during the preparation of this paper. Specif-
554 ically, LLMs were employed to assist in searching for related work, polishing the language of the
555 manuscript, and providing clarifications on background knowledge with which the authors were less
556 familiar. Importantly, LLMs did not contribute to the design of the research, the development of
557 the methodology, or the generation of research ideas. All content suggested by LLMs was carefully
558 reviewed and verified by the authors before inclusion in the final version of the paper.

559 As for polishing the language of the manuscript, every time the authors only input several sentences
560 or a short paragraph (rather than the whole draft) written by themselves to LLMs. When LLMs
561 returned the polished words, the authors reviewed the preciseness and authenticity of the contents
562 generated.

563 About searching for related work and background knowledge, every time the authors input a query
564 about the research area of interest and received a summary from LLMs. Then, the authors manually
565 and carefully checked the materials informed by LLMs, ensuring that LLMs only played the role as
566 an assistant or an intelligent search engine.

567
568 REFERENCES
569

570 Noa Agmon and Peter Stone. Leading ad hoc agents in joint action settings with multiple teammates.
571 In *AAMAS*, pp. 341–348, 2012.

572 Noa Agmon, Samuel Barrett, and Peter Stone. Modeling uncertainty in leading ad hoc teams. In
573 *Proceedings of the 2014 international conference on Autonomous agents and multi-agent systems*,
574 pp. 397–404, 2014.

576 Stefano V Albrecht and Subramanian Ramamoorthy. A game-theoretic model and best-response
577 learning method for ad hoc coordination in multiagent systems. In *Proceedings of the 2013*
578 *international conference on Autonomous agents and multi-agent systems*, pp. 1155–1156, 2013.

599 John F Banzhaf III. Weighted voting doesn't work: A mathematical analysis. *Rutgers L. Rev.*, 19:
580 317, 1964.

582 Ronen I Brafman and Moshe Tennenholtz. On partially controlled multi-agent systems. *Journal of*
583 *Artificial Intelligence Research*, 4:477–507, 1996.

584 Jiajun Chai, Yuqian Fu, Dongbin Zhao, and Yuanheng Zhu. Aligning credit for multi-agent coop-
585 eration via model-based counterfactual imagination. In *Proceedings of the 23rd International*
586 *Conference on Autonomous Agents and Multiagent Systems*, pp. 281–289, 2024.

588 Georgios Chalkiadakis, Edith Elkind, and Michael Wooldridge. *Computational aspects of cooperative*
589 *game theory*. Morgan & Claypool Publishers, 2011.

590 Junyoung Chung, Caglar Gulcehre, KyungHyun Cho, and Yoshua Bengio. Empirical evaluation of
591 gated recurrent neural networks on sequence modeling. *arXiv preprint arXiv:1412.3555*, 2014.

593 Paweł Cichosz. Truncating temporal differences: On the efficient implementation of td (lambda) for
reinforcement learning. *Journal of Artificial Intelligence Research*, 2:287–318, 1994.

594 Peter Dayan. The convergence of td (λ) for general λ . *Machine learning*, 8:341–362, 1992.
 595

596 Peter Dayan and Terrence J Sejnowski. Td (λ) converges with probability 1. *Machine Learning*, 14:
 597 295–301, 1994.

598 Christian Schroeder De Witt, Tarun Gupta, Denys Makoviichuk, Viktor Makoviychuk, Philip HS
 599 Torr, Mingfei Sun, and Shimon Whiteson. Is independent learning all you need in the starcraft
 600 multi-agent challenge? *arXiv preprint arXiv:2011.09533*, 2020.
 601

602 Pradeep Dubey. On the uniqueness of the shapley value. *International Journal of Game Theory*, 4(3):
 603 131–139, 1975.

604 Gianluigi Greco, Enrico Malizia, Luigi Palopoli, Francesco Scarcello, et al. On the complexity of the
 605 core over coalition structures. In *IJCAI*, volume 11, pp. 216–221, 2011.
 606

607 Lewis Hammond, Alan Chan, Jesse Clifton, Jason Hoelscher-Obermaier, Akbir Khan, Euan McLean,
 608 Chandler Smith, Wolfram Barfuss, Jakob Foerster, Tomáš Gavenčiak, et al. Multi-agent risks from
 609 advanced ai. *arXiv preprint arXiv:2502.14143*, 2025.
 610

611 Dongge Han, Chris Xiaoxuan Lu, Tomasz Michalak, and Michael Wooldridge. Multiagent model-
 612 based credit assignment for continuous control. *arXiv preprint arXiv:2112.13937*, 2021.

613 Dongge Han, Chris Xiaoxuan Lu, Tomasz Michalak, and Michael Wooldridge. Multiagent model-
 614 based credit assignment for continuous control. In *Proceedings of the 21st International Conference
 615 on Autonomous Agents and Multiagent Systems*, pp. 571–579, 2022.
 616

617 Jiahui Li, Kun Kuang, Baoxiang Wang, Furui Liu, Long Chen, Fei Wu, and Jun Xiao. Shapley
 618 counterfactual credits for multi-agent reinforcement learning. In *Proceedings of the 27th ACM
 619 SIGKDD Conference on Knowledge Discovery & Data Mining*, pp. 934–942, 2021.

620 Yang Li, Shao Zhang, Jichen Sun, Yali Du, Ying Wen, Xinbing Wang, and Wei Pan. Cooperative
 621 open-ended learning framework for zero-shot coordination. In Andreas Krause, Emma Brunskill,
 622 Kyunghyun Cho, Barbara Engelhardt, Sivan Sabato, and Jonathan Scarlett (eds.), *Proceedings of
 623 the 40th International Conference on Machine Learning*, volume 202 of *Proceedings of Machine
 624 Learning Research*, pp. 20470–20484. PMLR, 23–29 Jul 2023.
 625

626 Yang Li, Dengyu Zhang, Junfan Chen, Ying Wen, Qingrui Zhang, Shaoshuai Mou, and Wei Pan.
 627 Hola-drone: Hypergraphic open-ended learning for zero-shot multi-drone cooperative pursuit,
 628 2024.

629 Siddharth Nayak, Kenneth Choi, Wenqi Ding, Sydney Dolan, Karthik Gopalakrishnan, and Hamsa
 630 Balakrishnan. Scalable multi-agent reinforcement learning through intelligent information aggre-
 631 gation. In *International Conference on Machine Learning*, pp. 25817–25833. PMLR, 2023.
 632

633 Frans A Oliehoek, Christopher Amato, et al. *A concise introduction to decentralized POMDPs*,
 634 volume 1. Springer, 2016.

635 Jing Peng and Ronald J Williams. Incremental multi-step q-learning. In *Machine Learning Proceed-
 636 ings 1994*, pp. 226–232. Elsevier, 1994.
 637

638 Muhammad A Rahman, Niklas Hopner, Filippos Christianos, and Stefano V Albrecht. Towards open
 639 ad hoc teamwork using graph-based policy learning. In *International Conference on Machine
 640 Learning*, pp. 8776–8786. PMLR, 2021.

641 John Schulman, Philipp Moritz, Sergey Levine, Michael Jordan, and Pieter Abbeel. High-dimensional
 642 continuous control using generalized advantage estimation. *arXiv preprint arXiv:1506.02438*,
 643 2015.

644 Harm Seijen and Rich Sutton. True online td (lambda). In *International Conference on Machine
 645 Learning*, pp. 692–700. PMLR, 2014.

647 LS Shapley. A value for n-person games. *Annals of Mathematics Studies*, 28:307–318, 1953.

648 Peter Stone and Sarit Kraus. To teach or not to teach? decision making under uncertainty in ad hoc
 649 teams. In *Proceedings of the 9th International Conference on Autonomous Agents and Multiagent*
 650 *Systems: volume 1-Volume 1*, pp. 117–124, 2010.

651

652 Richard S Sutton. Learning to predict by the methods of temporal differences. *Machine learning*, 3:
 653 9–44, 1988.

654

655 Richard S Sutton and Andrew G Barto. Reinforcement learning: An introduction second edition.
 656 *Adaptive computation and machine learning: The MIT Press, Cambridge, MA and London*, 2018.

657

658 John Tsitsiklis and Benjamin Van Roy. Analysis of temporal-difference learning with function
 659 approximation. *Advances in neural information processing systems*, 9, 1996.

660

661 Caroline Wang, Muhammad Arrasy Rahman, Ishan Durugkar, Elad Liebman, and Peter Stone. N-
 662 agent ad hoc teamwork. *Advances in Neural Information Processing Systems*, 37:111832–111862,
 663 2025.

664

665 Jianhong Wang, Yuan Zhang, Tae-Kyun Kim, and Yunjie Gu. Shapley q-value: A local reward
 666 approach to solve global reward games. In *Proceedings of the AAAI conference on artificial*
 667 *intelligence*, volume 34, pp. 7285–7292, 2020.

668

669 Jianhong Wang, Wangkun Xu, Yunjie Gu, Wenbin Song, and Tim C Green. Multi-agent reinforcement
 670 learning for active voltage control on power distribution networks. *Advances in Neural Information*
 671 *Processing Systems*, 34:3271–3284, 2021.

672

673 Jianhong Wang, Yuan Zhang, Yunjie Gu, and Tae-Kyun Kim. Shaq: Incorporating shapley value
 674 theory into multi-agent q-learning. *Advances in Neural Information Processing Systems*, 35:
 675 5941–5954, 2022.

676

677 Jianhong Wang, Yang Li, Yuan Zhang, Wei Pan, and Samuel Kaski. Open ad hoc teamwork with
 678 cooperative game theory. In *International Conference on Machine Learning*, pp. 50902–50930.
 679 PMLR, 2024.

680

681 Christopher John Cornish Hellaby Watkins et al. Learning from delayed rewards. *PhD Thesis*, 1989.

682

683 David Williams. *Probability with martingales*. Cambridge university press, 1991.

684

685 Annie Xie, Dylan Losey, Ryan Tolsma, Chelsea Finn, and Dorsa Sadigh. Learning latent representa-
 686 tions to influence multi-agent interaction. In *Conference on robot learning*, pp. 575–588. PMLR,
 687 2021.

688

689 Di Xue, Lei Yuan, Zongzhang Zhang, and Yang Yu. Efficient multi-agent communication via shapley
 690 message value. In *IJCAI*, pp. 578–584, 2022.

691

692 H Peyton Young. Monotonic solutions of cooperative games. *International Journal of Game Theory*,
 693 14(2):65–72, 1985.

694

695 Chao Yu, Akash Velu, Eugene Vinitsky, Jiaxuan Gao, Yu Wang, Alexandre Bayen, and Yi Wu. The
 696 surprising effectiveness of ppo in cooperative multi-agent games. *Advances in neural information*
 697 *processing systems*, 35:24611–24624, 2022.

698

699 Yuan Zhang, Umashankar Deekshith, Jianhong Wang, and Joschka Boedecker. Improving the
 700 efficiency and efficacy of multi-agent reinforcement learning on complex railway networks with a
 701 local-critic approach. In *Proceedings of the International Conference on Automated Planning and*
Scheduling, volume 34, pp. 698–706, 2024.

702

703 Luisa M. Zintgraf, Sam Devlin, Kamil Ciosek, Shimon Whiteson, and Katja Hofmann. Deep
 704 interactive bayesian reinforcement learning via meta-learning. In Frank Dignum, Alessio Lomuscio,
 705 Ulle Endriss, and Ann Nowé (eds.), *AAMAS '21: 20th International Conference on Autonomous*
Agents and Multiagent Systems, Virtual Event, United Kingdom, May 3-7, 2021, pp. 1712–1714.
 706 ACM, 2021. doi: 10.5555/3463952.3464210.

702 A RELATED WORK
703704 A.1 TD(λ) IN REINFORCEMENT LEARNING AND MULTI-AGENT REINFORCEMENT LEARNING
705

706 Related work on temporal-difference learning with eligibility traces centers on the seminal TD(λ)
707 algorithm proposed by Sutton (1988), which unified one-step TD and Monte Carlo methods via a trace-
708 decay parameter λ and introduced the forward- and backward-view equivalence for efficient multi-
709 step credit assignment. Subsequent theoretical analyses (Dayan, 1992; Dayan & Sejnowski, 1994;
710 Tsitsiklis & Van Roy, 1996) established convergence guarantees and characterized the bias-variance
711 trade-off inherent in λ -returns, while extensions by Watkins et al. (1989); Peng & Williams (1994)
712 adapted eligibility traces for off-policy control, Q(λ). Advances in function approximation, including
713 true online TD(λ) (Seijen & Sutton, 2014) and gradient-TD methods, further broadened applicability
714 to large-scale and nonlinear settings, inspiring n-step return techniques such as generalized advantage
715 estimation (GAE) (Schulman et al., 2015) for policy optimization. In multi-agent reinforcement
716 learning, algorithms of PPO family such as MAPPO (Yu et al., 2022) and IPPO (De Witt et al., 2020),
717 applied GAE to optimize policies and thus used TD(λ) as the target values to train critics. This
718 paper highlights the theoretical link between truncated TD(λ), denoted TTD(λ) (Cichosz, 1994), in
719 NAHT (a generalization of MARL) and the axioms of the Shapley value. It further shows that the
720 number of n -step return components in TTD(λ) can be determined by the number of agents. This
721 insight provides a theoretical foundation that could inform the design of a broader class of multi-agent
722 reinforcement learning algorithms.

723 A.2 THEORETICAL MODELS FOR AD HOC TEAMWORK
724

725 We now discuss theoretical models describing ad hoc teamwork (AHT). Brafman & Tennenholz
726 (1996) pioneered research into AHT by investigating repeated matrix games involving a single
727 teammate. Subsequent studies expanded this framework to scenarios with multiple teammates,
728 notably by Agmon & Stone (2012). Later, Agmon et al. (2014) further relaxed earlier assumptions
729 by allowing teammates' policies to be selected from a known set. Stone et al. Stone & Kraus
730 (2010) initially formalized AHT through collaborative multi-armed bandits, albeit under notable
731 assumptions such as prior knowledge of teammates' policies and environmental conditions. Albrecht
732 & Ramamoorthy (2013) advanced this field significantly by introducing the stochastic Bayesian
733 game (SBG), the first comprehensive theoretical framework accommodating dynamic environments
734 and unknown teammate behaviours in AHT. Building on SBG, Rahman et al. (2021) proposed the
735 open stochastic Bayesian game (OSBG), addressing open ad hoc teamwork (OAHT). Zintgraf et al.
736 (2021) modelled AHT through interactive Bayesian reinforcement learning (IBRL) within Markov
737 games, specifically targeting non-stationary teammate policies within single episodes. Xie et al.
738 (2021) introduced the hidden parameter Markov decision process (HiP-MDP) to handle situations
739 where teammates' policies vary across episodes but remain stationary during individual episodes.
740 Most recently, Wang et al. (2024) extended OSBG by incorporating principles from cooperative
741 game theory, introducing the open stochastic Bayesian coalitional affinity game (OSBG-CAG),
742 which theoretically justifies a graph-based representation for joint Q-value functions and includes
743 rigorous convergence proofs for Q-learning algorithms in open team settings. This paper adopts the
744 perspective of cooperative game theory, introducing an axiomatic framework based on state-specific
745 cooperative games to address the NAHT problem. Within this framework, the Shapley value's
746 axioms are extended and enforced, so that Shapley-based algorithms emerge implicitly by satisfying
747 these axioms during learning. More importantly, this axiomatic characterization also motivates a
748 new algorithm, the Banzhaf Machine, which preserves the advantages of the Shapley value while
749 alleviating some of its limitations.

750 A.3 SHAPLEY VALUE IN MULTI-AGENT REINFORCEMENT LEARNING
751

752 Related work mainly focused on developing the theory of Shapley value in MARL, and incorporated
753 Shapley value (Shapley, 1953) into MARL algorithms. Early studies (Wang et al., 2020) incorporated
754 Shapley value into credit assignment scheme in a principled way and proposed an algorithm named
755 SQDDPG, underpinned by the equivalence between cooperative-game theoretical models in dynamic
scenarios and the shared reward Markov games. Wang et al. (2022) further improved the theory
by proving the existence of Shapley value, and proposed an algorithm named SHAQ, an algorithm
with promising convergence to find an optimal joint policy. It also shed light on the relationship

756 between Shapley value and the relevant value decomposition and credit assignment approaches for
 757 MARL. Li et al. (2021) improved the stability of SQDDPG and proposed an algorithm named Shapley
 758 Counterfactual Credits. Han et al. (2021) incorporated Shapley value into the model-based PPO as
 759 each agent’s advantage value, and estimated coalition values by trained transition and reward models.
 760 Chai et al. (2024) continued the idea from Han et al. (2021), by replacing the the transition and
 761 reward models with more powerful world models. Xue et al. (2022) incorporated Shapley value into
 762 multi-agent communication, as a criterion for forming communication between agents. This paper
 763 primarily focuses on learning the Shapley value to address the NAHT, a generalized paradigm to
 764 MARL. More importantly, the Shapley values are learned by complying with their axioms, rather than
 765 by constructing their explicit formulas as implemented in the previous work. This may help overcome
 766 the notorious learning instability issues caused by learning substantial “coalitional values” in the
 767 existing algorithms based on Shapley values. Furthermore, the insight of axiomatic characterization
 768 can facilitate the flexibility of Shapley value approaches in a wide variety of tasks. Specifically, one
 769 can safely drop any part of a learning algorithm, if it is justified that the targeting task does not align
 770 with the corresponding axiom.

771 B EXTRA BACKGROUND

772 B.1 λ -RETURN AND TD(λ)

773 We now introduce an extension of return named λ -return. Mathematically, a λ -return G_t^λ for infinite-
 774 horizon cases can be expressed as follows:

$$775 \begin{aligned} G_{t:t+n} &= R_t + \gamma R_{t+1} + \cdots + \gamma^{n-1} R_{t+n-1} + \gamma^n V(s_{t+n}), \\ 776 G_t^\lambda &= (1 - \lambda) \sum_{n=1}^{\infty} \lambda^n G_{t:t+n}. \end{aligned} \quad (12)$$

777 Similarly, the λ -return for finite-horizon cases can be expressed as follows:

$$778 \begin{aligned} G_t^\lambda &= (1 - \lambda) \sum_{n=1}^{T-t} \lambda^n G_{t:t+n} + \lambda^{T-t} G_{t:T}. \end{aligned} \quad (13)$$

779 Note that if $\lambda = 1$, updating according to the λ -return is a Monte Carlo algorithm. In contrast, if
 780 $\lambda = 0$, then the λ -return reduces to $G_{t:t+1}$, the one-step return. Monte Carlo algorithm is known as
 781 its high variance but low bias, while one-step return is known as its low variance but high bias. For
 782 this reason, the change of λ can be seen as a tradeoff between bias and variance. The TD prediction
 783 using λ -return as the target value is referred to as TD(λ) (Sutton, 1988).

784 **A variant of TD(λ) by shaping G_t^λ with a designated horizon $t < H \leq T$ is referred to as
 785 truncated TD(λ), shortened as TTD(λ) (Cichosz, 1994).** Mathematically, G_t^λ with a designated
 786 horizon H can be formulated as follows:

$$787 \begin{aligned} G_t^\lambda &= (1 - \lambda) \sum_{n=1}^{H-t} \lambda^n G_{t:t+n} + \lambda^{H-t} G_{t:H}. \end{aligned} \quad (14)$$

788 Note that in the convention of RL, the horizon H is defined as the time difference from the starting
 789 point of an episode, denoted by $t = 0$.

790 **Remark B.1.** *In this paper, to simply the presentation of our work, we redefine the horizon as the
 791 time difference from each timestep t , denoted as m , such that $m = H - t$. With the new definition of
 792 horizon, we can rewrite the above formula of G_t^λ as follows:*

$$793 \begin{aligned} G_t^\lambda &= (1 - \lambda) \sum_{n=1}^m \lambda^n G_{t:t+n} + \lambda^m G_{t:t+m}. \end{aligned} \quad (15)$$

807 B.2 SUPERADDITIVE GAME AND COOPERATIVE MULTI-AGENT REINFORCEMENT LEARNING

808 The superadditive game is a subclass of characteristic games that satisfies an additional condition:
 809 $v(C \cup D) \geq v(C) + v(D)$, for any two distinct coalitions $C, D \subseteq \mathcal{M}$ with $C \cap D = \emptyset$. Previous

work in MARL (Wang et al., 2020) has shown the equivalence on the task objective function between state-based superadditive games with action space and team reward Markov games with coalition structures.⁴ Intuitively, the Shapley value is a solution to the stability of a team formation, resembling cooperation. Since the NAHT is a generalization of MARL, this conclusion still valid in principle. It has been already proved that the Shapley value exists in superadditive games (Shapley, 1953) and each game instance in superadditive games can be uniquely represented as $\sum k_C v_C^1$, where $k_C \geq 0$ (Dubey, 1975). In the cooperative game theory, any game can be transformed to a superadditive game if its value v is transformed by a *superadditive cover* v^* such that $v^*(C) = \max_{CS(C)} \sum_{D \in CS(C)} v(D)$ (Greco et al., 2011). As a result, **it will not lose generality if we consider the cooperative game space as superadditive games in this paper.**

B.3 BASELINE ALGORITHMS: POAM AND IPPO

POAM. In general, POAM is an algorithm built upon IPPO (De Witt et al., 2020). The primary difference between POAM and IPPO is as follows: **For each agent’s policy and value, in addition to its observation used in IPPO, POAM takes as input an embedding vector to predict other agents’ potential behaviours.** More specifically, this embedding vector is trained by an encoder-decoder structure, wherein the encoder is modeled as RNNs and decoder is modeled as MLPs. For brevity, $-i$ denotes the set of all agents excluding agent i . Let $h_{t,i} = \{o_{k,i}, a_{k-1,i}\}_{k=1}^t$ denote agent i ’s history of observations and actions up to timestep t and $e_{t,i} \in \mathbb{R}^n$ denote the resulting embedding vector of n dimensions. The encoder parameterized by θ^e is defined as $f_{\theta^e}^{enc} : \mathcal{H}_i \rightarrow \mathbb{R}^n$. The embedding vector is decoded by two decoder networks: the observation decoder $f_{\theta^o}^{dec} : \mathbb{R}^n \rightarrow \mathcal{O}_{-i}$, and the action decoder $f_{\theta^a}^{dec} : \mathbb{R}^n \rightarrow \Delta(\mathcal{A}_{-i})$. The decider networks are respectively trained to predict the observations and actions of all other agents on the team at timestep t , $o_{t,-i}$ and $a_{t,-i}$, to encourage $e_{t,i}$ to contain information about collective behaviors corresponding to $h_{t,i}$. While the observation decoder directly predicts the observed $-i$ ’s observations, the action decoder predicts the parameters of a probability distribution over the $-i$ ’s actions $\pi_{-i}(a_{t,-i}; f_{\theta^a}^{dec}(f_{\theta^e}^{enc}(h_{t,i})))$. As we consider continuous observations and discrete actions, the loss function with using categorical distribution to model π_{-i} is as follows:

$$L_{\theta^e, \theta^o, \theta^a}(h_{t,i}, o_{t,-i}, a_{t,-i}) = \|f_{\theta^o}^{dec}(f_{\theta^e}^{enc}(h_{t,i})) - o_{t,-i}\|^2 - \log \pi_{-i}(a_{t,-i}; f_{\theta^a}^{dec}(f_{\theta^e}^{enc}(h_{t,i}))). \quad (16)$$

For brevity, we define $g(h) := (h, f_{\theta^e}^{enc}(h))$ in the following description.

POAM employed generalized advantage estimation (GAE) (Schulman et al., 2015) to form the policy gradient, and the value function used to form GAE is trained by the following loss function:

$$L_{\theta^c}(h_{t,i}) = \frac{1}{2} \left(V_i^{\theta^c}(g(h_{t,i})) - \hat{V}_{t,i} \right)^2, \quad (17)$$

where $\hat{V}_{t,i}$ is the finite-horizon TD(λ) return, for which the horizon is up to the episode length T . Each agent i ’s GAE estimation is as follows:

$$A_{t,i} = \sum_{l=0}^T (\gamma \lambda)^l \delta_{t+l,i}, \quad (18)$$

where $\delta_{t,i} = R_t + \gamma V_i(g(h_{t,i})) - V_i^{\theta^c}(g(h_{t,i}))$ and $V_i(g(h_{t,i}))$ denotes the non-parameterized individual value. Based on the GAE defined above, the policy optimization loss is defined as:

$$L_{\theta}(h_{t,i}, a_{t,i}) = \min \left\{ \frac{\pi_{\theta}(a_{t,i}|g(h_{t,i}))}{\pi_{\theta_{old}}(a_{t,i}|g(h_{t,i}))} A_{t,i}, \text{clip} \left(\frac{\pi_{\theta}(a_{t,i}|g(h_{t,i}))}{\pi_{\theta_{old}}(a_{t,i}|g(h_{t,i}))}, 1 - \epsilon, 1 + \epsilon \right) A_{t,i} \right\}. \quad (19)$$

IPPO. By removing the loss for the encoder-decoder structure as shown in Eq. 16 and replacing the input $g(h_{t,i})$ by $h_{t,i}$ in the above set of equations, we get the loss functions of IPPO.

⁴In Wang et al. (2020), state-based convex games with action space were proved to be equivalent to team reward Markov games. However, setting $C \cap D = \emptyset$ can relax a convex game to a superadditive game.

864 **C JUSTIFICATION AND DISCUSSION OF SIZE-LEXICOGRAPHIC COALITION**
 865 **ORDER AND HORIZON ASSIGNMENT**
 866

867 In this section, we will justify the insight behind the size-lexicographic coalition order and horizon
 868 assignment, as shown in Definition 4.4. In the beginning, we define a discrete-time stochastic process
 869 of TD error terms $(Z_n)_{n \in \mathbb{N}_0}$, where $v_\pi(s_t)$ denotes a generic state value function:
 870

871 $Z_{n+1} := R_{t+n} + \gamma v_\pi(s_{t+n+1}) - v_\pi(s_{t+n}), \quad \text{so} \quad G_{t:t+n+1} = G_{t:t+n} + \gamma^n Z_{n+1}.$
 872

873 We first show a generic result related to the one-step increment term in Lemma C.1. Then, we
 874 make the coalition-variance monotonicity assumption in Assumption C.2, which can be justified by
 875 Remark C.3, **with evidence from the basis game values of the game-structured NAHT**, as shown
 876 in Definition 3.2. By Lemma C.1 and Assumption C.2, we get that for the coalition enumeration
 877 $\{i\}$ there exist nondecreasing orderings of variances for both the sequence of basis game values
 878 of coalitions nondecreasing by sizes and the sequence of n-step returns with the horizon schedule
 879 $n_i = n_{i-1} + 1$. This motivates that we can define the following term under this **monotone-variance**
 880 **regularity**:

881 $V(C_i, s) := \mathbb{E}_\pi[G_{t:t+n_i} \mid s_t = s], \quad (i = 1, \dots, m).$
 882

883 The justification of Definition 4.4 completes.
 884

885 Remark C.5 highlights that alternative horizon schedules (e.g., $n_i = n_{i-1} + k$, $n_1 = 1, k > 0$) can
 886 be incorporated, offering additional design possibilities within our axiomatic framework.
 887

888 **Lemma C.1.** *If (Z_n) has nonnegative autocovariances given $s_t = s$, then $n \mapsto \text{Var}(G_{t:t+n} \mid s)$ is
 889 nondecreasing, with $\text{Var}(G_{t:t+n+1} \mid s) = \text{Var}(G_{t:t+n} \mid s)$ iff $\text{Var}(Z_{n+1} \mid s) = 0$.*
 890

891 *Proof.* Use $G_{t:t+n+1} = G_{t:t+n} + \gamma^n Z_{n+1}$ and expand the variance conditioning on $s_t = s$, we can
 892 get the following formula:
 893

894 $\text{Var}(G_{t:t+n+1} \mid s) = \text{Var}(G_{t:t+n} \mid s) + 2\gamma^n \text{Cov}(G_{t:t+n}, Z_{n+1} \mid s) + \gamma^{2n} \text{Var}(Z_{n+1} \mid s).$
 895

896 **We prove if (Z_n) has nonnegative autocovariances given $s_t = s$, then $n \mapsto \text{Var}(G_{t:t+n} \mid s)$ is
 897 nondecreasing.**

898 Using the sum of TD errors to represent the Monte Carlo error (Sutton & Barto, 2018)[Chap. 6], we
 899 have the following formula:
 900

901
$$G_{t:t+n} - v_\pi(s_t) = \sum_{k=0}^{n-1} \gamma^k Z_{k+1}.$$

 902

903 Given the linear property of covariance and a fact that the covariance of a constant is zero, we can get:
 904

905
$$\text{Cov}(G_{t:t+n}, Z_{n+1} \mid s) = \sum_{k=0}^{n-1} \gamma^k \text{Cov}(Z_{k+1}, Z_{n+1} \mid s).$$

 906

907 Therefore, **if all autocovariances $\text{Cov}(Z_i, Z_j \mid s) \geq 0$, then $\text{Cov}(G_{t:t+n}, Z_{n+1} \mid s) \geq 0$.**
 908

909 Since $\text{Var}(Z_{n+1} \mid s) \geq 0$ must hold, we can directly get:
 910

911
$$\text{Var}(G_{t:t+n+1} \mid s) \geq \text{Var}(G_{t:t+n} \mid s).$$

 912

913 That is, $n \mapsto \text{Var}(G_{t:t+n} \mid s)$ is nondecreasing.
 914

915 **We prove $\text{Var}(G_{t:t+n+1} \mid s) = \text{Var}(G_{t:t+n} \mid s)$ iff $\text{Var}(Z_{n+1} \mid s) = 0$.**
 916

917 It is a fact that $\text{Var}(G_{t:t+n+1} \mid s) = \text{Var}(G_{t:t+n} \mid s)$ iff

918
$$\text{Var}(Z_{n+1} \mid s) = 0, \quad \text{Cov}(G_{t:t+n}, Z_{n+1} \mid s) = 0.$$

 919

920 We aim to prove that $\text{Var}(Z_{n+1} \mid s) = 0$ is sufficient for $\text{Cov}(G_{t:t+n}, Z_{n+1} \mid s) = 0$.
 921

If a nonnegative random variable (r.v.) $W \geq 0$ satisfies $\mathbb{E}[W | s] = 0$, then $W = 0$ almost surely (a.s.) given s (Williams, 1991)[Chap. 9].

Apply this with $W = (Z_{n+1} - \mathbb{E}[Z_{n+1} | s])^2$. If $\text{Var}(Z_{n+1} | s) = 0$, then

$$\mathbb{E}[(Z_{n+1} - \mathbb{E}[Z_{n+1} | s])^2 | s] = 0 \Rightarrow (Z_{n+1} - \mathbb{E}[Z_{n+1} | s])^2 = 0 \text{ a.s.} \Rightarrow Z_{n+1} = \mathbb{E}[Z_{n+1} | s] \text{ a.s.}$$

The covariance $\text{Cov}(G_{t:t+n}, Z_{n+1} | s)$ can be expressed as the following formula:

$$\text{Cov}(G_{t:t+n}, Z_{n+1} | s) = \mathbb{E}[(G_{t:t+n} - \mathbb{E}[G_{t:t+n} | s])(Z_{n+1} - \mathbb{E}[Z_{n+1} | s]) | s].$$

Since $Z_{n+1} - \mathbb{E}[Z_{n+1} | s] = 0$ a.s., we get the following result:

$$\text{Cov}(G_{t:t+n}, Z_{n+1} | s) = 0.$$

□

Assumption C.2 (Coalition-Variance Monotonicity). Let $\widehat{V}(C, s)$ be an unbiased estimator of $v_\pi(s)$ from on-policy data restricted to agents in C . Assume $\text{Var}(\widehat{V}(C, s))$ is nondecreasing in $|C|$ (larger coalitions \Rightarrow richer interactions \Rightarrow higher variance).

Remark C.3 (Coalition-Variance Monotonicity in Game-Structured NAHT). Recall from Section 4.1 that $v_{C,s}^{v_s(\mathcal{M})} = v_s(\mathcal{M})v_{C,s}^1$, and $v_{C,s}^1$ in a given state s is isomorphic to v_C^1 . Following Definition 2.1, we can express $v_{C,s}^{v_s(\mathcal{M})}$ as follows:

$$v_{C,s}^{v_s(\mathcal{M})}(D) = \begin{cases} v_s(\mathcal{M}) & \text{if } C \subseteq D, \\ 0 & \text{otherwise.} \end{cases}$$

As described in Definition 3.2, a basis game value $v_{C,s}^{v_s(\mathcal{M})}(D)$ can effectively evaluate the performance of a team of agents C^5 with an agent-type composition denoted by $\times_{i \in D} T_i$, where T_i indicates the agent i 's type.

As the size of the coalition C increases, it requires more experience for exploring agent-type compositions during agent interactions, so that the value of $V(C, s) := v_{C,s}^{v_s(\mathcal{M})}(\mathcal{M})$ can predict $v_s(\mathcal{M})$. It implies that as the coalition size increases, higher variance of the value prediction is incurred to get $v_s(\mathcal{M})$, due to the growing agent-type composition space. Similarly, if the sizes of two coalition are equal, their variances are equal.

Proposition C.4 (Variance Monotonicity along the Coalition Enumeration). Fix $s \in \mathcal{S}$ and the sequence (C_i, n_i) of Definition 4.4. Under the nonnegative-autocovariance condition of Lemma C.1 and Assumption C.2, the sequences

$$i \mapsto \text{Var}(\widehat{V}(C_i, s)) \quad \text{and} \quad i \mapsto \text{Var}(G_{t:t+n_i} | s)$$

are both nondecreasing in i . Moreover, $i \mapsto \text{Var}(G_{t:t+n_i} | s)$ is strictly increasing at every index where $\text{Var}(Z_{n_i+1} | s) > 0$.

Proof. Since $n_i = n_{i-1} + 1$ is strictly increasing, Lemma C.1 yields nondecreasing variance in i , with strictness when the added step contributes nonzero variance. Assumption C.2 gives nondecreasing $\text{Var}(\widehat{V}(C_i, s))$ as $|C_i|$ (hence i) increases. □

Remark C.5 (Minimality of Horizon Schedule). Among all sequences (\tilde{n}_i) with $\tilde{n}_1 = 1$, $\tilde{n}_i > \tilde{n}_{i-1}$, and $\tilde{n}_i \geq |C_i|$ for all i , the schedule in Definition 4.4 is pointwise minimal: $\tilde{n}_i \geq n_i$ for every i .

⁵For any team of agents $D \supset C$, the basis game value would be the same as $v_{C,s}^{v_s(\mathcal{M})}(C)$, so it is ineffective to evaluate the performance of the D with the larger size than C .

972 **D COMPLETE MATHEMATICAL PROOFS**
 973

974 **Lemma 4.1.** *Given a fixed state $s \in \mathcal{S}$, each state-specific cooperative game's value $v_s \in \mathcal{G}(s)$ can*
 975 *be uniquely represented by: $v_s = \sum_{\emptyset \neq C \subseteq \mathcal{M}} k'_C \cdot v_{C,s}^z$, where $k'_C = \frac{k_C}{z}$ and $z \neq 0$.*
 976

977 *Proof.* We can represent each k_C in an equivalent form as $\frac{k_C \cdot z}{z}$, where $z \neq 0$. Substituting this term
 978 into the formula $v_s = \sum_{\emptyset \neq C \subseteq \mathcal{M}} k_C v_{C,s}^1$ in Definition 2.1, we can get the following formula such
 979 that:
 980

$$981 \quad v_s = \sum_{\emptyset \neq C \subseteq \mathcal{M}} \frac{k_C \cdot z}{z} \cdot v_{C,s}^1.$$

983 Since $v_{C,s}^z = z \cdot v_{C,s}^1$ by Definition 2.1, we have the following formula such that:
 984

$$985 \quad v_s = \sum_{\emptyset \neq C \subseteq \mathcal{M}} \frac{k_C}{z} \cdot v_{C,s}^z.$$

□

989 **Proposition 4.2.** *For the class of superadditive games formed by a set of basis games $\{v_{C,s}^z | \emptyset \neq C \subseteq \mathcal{M}\}$, it holds that $k_C \geq 0$, for all $\emptyset \neq C \subseteq \mathcal{M}$.*
 990

992 *Proof.* We first consider a cooperative game space \mathcal{G} (a broader space of superadditive games). As
 993 per Dubey (1975), a game $v : \mathcal{G} \rightarrow \mathbb{R}_{\geq 0}$ belonging to \mathcal{G} can be uniquely represented as follows:
 994

$$995 \quad v = \sum_{\emptyset \neq C \subseteq \tilde{N}} k_C v_C^1.$$

998 The analytic form of k_C under \mathcal{G} is represented as follows:
 999

$$1000 \quad k_C = \sum_{T \subseteq C} (-1)^{|C|-|T|} v(T).$$

1003 The condition for v to be a superadditive game is as follows:
 1004

$$1005 \quad v(T_1 \cup T_2) \geq v(T_1) + v(T_2), \quad T_1, T_2 \subseteq C.$$

1007 Following the result from Dubey (1975), if the above condition holds, $k_C \geq 0$ has to be satisfied.⁶

1008 We now extend the \mathcal{G} to a state-specific cooperative game space $\mathcal{G}(s)$, for a fixed state $s \in \mathcal{S}$. Since
 1009 the $\mathcal{G}(s)$ is isomorphic to a game space \mathcal{G} , the characteristics satisfied in the \mathcal{G} also holds in the $\mathcal{G}(s)$
 1010 by Remark 3.1. Therefore, $v_s : \mathcal{G}(s) \rightarrow \mathbb{R}_{\geq 0}$ can be uniquely represented as $v_s = \sum_{\emptyset \neq C \subseteq \mathcal{M}} k_C v_{C,s}^1$.
 1011 As we consider $\mathcal{G}(s)$ as a space of superadditive games, $k_C \geq 0$ should hold.
 1012

1013 By Lemma 4.1, we have $v_s = \sum_{\emptyset \neq C \subseteq \mathcal{M}} k'_C \cdot v_{C,s}^z$, where $k'_C = \frac{k_C}{z}$ and $z \neq 0$. This implies that
 1014 any set of basis games in the form $\{v_{C,s}^z | \emptyset \neq C \subseteq \mathcal{M}\}$ can form a state-specific cooperative game
 1015 belonging to superadditive games. □

1016 **Proposition 4.6 (Representation of Transformed Rewards).** *Given the condition $\sum_{i=1}^M \phi_i(R_t) =$
 1017 R_t , the payoff allocation defined on rewards R_t , can be expressed as:*
 1018

$$1019 \quad \phi_i(R_t) := R_t - \sum_{j \neq i} (\phi_j(V(\mathcal{M}, s_t)) - \gamma \phi_j(V(\mathcal{M}, s_{t+1}))).$$

1022 *Proof.* Recall that $\phi(\cdot) \in \mathbb{R}^M$ is a multidimensional linear transformation, where M is the number
 1023 of agents. We now express $\phi(R_t)$ by introducing the Efficiency axiom.
 1024

1025 ⁶For example, if $C = \{1, 2\}$, then $T = \emptyset, \{1\}, \{2\}, \{1, 2\}$. As a result, $k_C = v(\emptyset) - v(\{1\}) - v(\{2\}) + v(\{1, 2\})$, where $v(\emptyset) = 0$ by default. If v is assumed to be a superadditive game, $k_C \geq 0$ has to hold.

1026 To satisfy the Efficiency axiom such that $\sum_{i=1}^M \phi_i(V(\mathcal{M}, s_t)) = V(\mathcal{M}, s_t)$, it is reasonable to
 1027 assume that $\sum_{i=1}^M \phi_i(R_t) = R_t$. In other words, each agent's value expansion can be expressed
 1028 independently in its own $\phi_i(R_t)$, justified by Theorem 4.7.
 1029

1030 Next, we aim to show how each $\phi_i(R_t)$ is expressed in terms of $\phi(V(\mathcal{M}, s_t))$.
 1031

1032 It is not difficult to observe that for each agent $i \in \mathcal{M}$, we have
 1033

$$\phi_i(V(\mathcal{M}, s_t)) = \phi_i(R_t) + \gamma \phi_i(V(\mathcal{M}, s_{t+1})).$$

1034 By the condition $\sum_{i=1}^M \phi_i(R_t) = R_t$, we can derive a formula such that:
 1035

$$\phi_i(R_t) = R_t - \sum_{j \neq i} \phi_j(R_t).$$

1039 Since $\phi_j(R_t) = \phi_j(V(\mathcal{M}, s_t)) - \gamma \phi_j(V(\mathcal{M}, s_{t+1}))$, we can express $\phi_i(R_t)$ as follows:
 1040

$$\phi_i(R_t) := R_t - \sum_{j \neq i} (\phi_j(V(\mathcal{M}, s_t)) - \gamma \phi_j(V(\mathcal{M}, s_{t+1}))).$$

1041 **Theorem 4.8.** *The payoff allocation operator satisfying permutation-equivariance is a sufficient
 1042 condition for the Symmetry axiom.*
 1043

1044 *Proof.* Let $\mathcal{M} = \{1, \dots, M\}$. Let \mathcal{G} be the set of cooperative games $v : 2^{\mathcal{M}} \rightarrow \mathbb{R}$, and S_C be a
 1045 permutation group acting on $C \subseteq \mathcal{M}$.
 1046

1047 Let S_C act on an arbitrary $C \subseteq \mathcal{M}$ by exchanging agents:
 1048

$$(\sigma \cdot v)(C) := v(\sigma^{-1}(C)), \quad \sigma \in S_{\mathcal{M}}, C \subseteq \mathcal{M}.$$

1049 Let a payoff allocation operator $F : \mathcal{G} \rightarrow \mathbb{R}^M$ output payoffs $F(v) = (F_1(v), \dots, F_n(v))$.
 1050

1051 Let $S_{\mathcal{M}}$ act on \mathbb{R}^M by permuting coordinates: $(\sigma \cdot x)_i := x_{\sigma^{-1}(i)}$.
 1052

1053 F is permutation-equivariant if
 1054

$$F(\sigma \cdot v) = \sigma \cdot F(v), \quad \forall \sigma \in S_{\mathcal{M}}, v \in \mathcal{G}. \quad (20)$$

1055 Recall that agents i and j are symmetric in v if
 1056

$$v(C \cup \{i\}) = v(C \cup \{j\}) \quad \forall C \subseteq \mathcal{M} \setminus \{i, j\}.$$

1057 Equivalently, the transposition $\tau = (i \ j)$ leaves the game value invariant:
 1058

$$\tau \cdot v = v. \quad (21)$$

1059 **Next, we aim to show $F_i(v) = F_j(v)$ to prove the statement in the theorem.**
 1060

1061 By Eqs. 20 and 21, we have
 1062

$$F(v) = F(\tau \cdot v) = \tau \cdot F(v).$$

1063 Note that $\tau \cdot F(v)$ is just $F(v)$ with coordinates i and j swapped. Therefore, $F(v) = \tau \cdot F(v)$ implies
 1064 the i -th and j -th entries are equal:
 1065

$$F_i(v) = F_j(v).$$

1066 \square

1080 **Theorem 4.10.** *Shapley Machine is an algorithm enforcing V_i to fulfil Efficiency, Symmetry and*
 1081 *Linearity, so the V_i is the Shapley value for dynamic scenarios.*

1083 *Proof.* By construction, the Shapley Machine enforces the individual value functions V_i (payoff
 1084 allocation functions) to satisfy the axioms of Efficiency, Symmetry, and Linearity. Each state-specific
 1085 cooperative game space $\mathcal{G}(s)$ is isomorphic to the canonical cooperative game space \mathcal{G} (Remark 3.1).
 1086 Hence, properties of payoff allocation functions that hold on \mathcal{G} also hold on $\mathcal{G}(s)$.

1087 Now, recall that the Shapley value is uniquely characterized as the value function that satisfies
 1088 Efficiency, Symmetry, and Additivity (Theorem 2.2). Since Linearity is a stronger condition than
 1089 Additivity (indeed, setting all $\alpha_i = 1$ in the definition of Linearity yields Additivity), any payoff
 1090 allocation function that is Efficient, Symmetric, and Linear must coincide with the Shapley value.
 1091 Therefore, the individual value functions V_i produced by the Shapley Machine are exactly the Shapley
 1092 values for dynamic scenarios. \square

1094 E EXPERIMENTAL DETAILS

1096 E.1 IMPLEMENTATION DETAILS

1098 Our algorithm is built upon POAM and IPPO. All loss functions for training the encoder-decoder
 1099 model, policy networks and value networks have been remained. Please refer to Appendix B.3 for
 1100 details. For conciseness, we only list the novel loss functions proposed in this paper as below.

1102 E.1.1 SHAPLEY MACHINE

1104 We now describe the details about implementing our proposed algorithm, referred to as Shapley
 1105 Machine. In general, our algorithm is established based on the base algorithms POAM and IPPO,
 1106 with modification to fulfil all the three axioms of Shapley value: Efficiency, Linearity and Symmetry.
 1107 Since Symmetry has been implemented by structuring the inputs as shown in Remark 4.9, we only
 1108 need to fulfil Efficiency and Linearity as follows.

1109 **Implementing the Linearity Axiom.** In general, both POAM and IPPO have implemented $TD(\lambda)$,
 1110 which does not strictly conform to the principle of the Linearity axiom. To this end, we change
 1111 the $TD(\lambda)$ to $TTD(\lambda)$, where the number of n -step return components is equal to the number of the
 1112 non-empty coalitions in theory. Note that in some scenarios the episode length is smaller than the
 1113 number of non-empty coalitions. In these cases, the $TTD(\lambda)$ can be reduced to the $TD(\lambda)$ for the
 1114 finite-horizon tasks with the episode length as T , equivalently, the $TTD(\lambda)$ with $m = T$. Alternatively,
 1115 we can select a value of m for each task based on extra conditions, which is left for the future work.
 1116 In this paper, we set $m = T$ for the scenarios 8v9 and 10v11. For the 8v9 scenario, the episode length
 1117 as 120 is not too far from the number of non-empty coalitions as 127. For the 10v11 scenario, the
 1118 episode length is 150, while the number of non-empty coalitions is 511.

1119 **Implementing the Efficiency Axiom.** By introducing the partial observation in Dec-POMDP, the
 1120 Eq. 10 we have derived the condition for realizing the Efficiency axiom is transformed as follows:

$$1121 \quad R_{t,i} = R_t - \sum_{j \neq i} (V_j(h_{t,j}) - \gamma V_j(h_{t+1,j})),$$

1124 where $V_j(h_{t,j})$ indicates an agent j 's non-parameterized individual value. During the practical training
 1125 procedure, the $V_j(h_{t,j})$ generated by the individual value network could be severely inaccurate in
 1126 the beginning, which may result in the instability of learning. To mitigate this issue, we add an extra
 1127 coefficient $\alpha \in (0, 1)$ to the term $\sum_{j \neq i} (V_j(h_{t,j}) - \gamma V_j(h_{t+1,j}))$, such that:

$$1129 \quad R_{t,i} = R_t - \alpha \sum_{j \neq i} (V_j(h_{t,j}) - \gamma V_j(h_{t+1,j})). \quad (22)$$

1131 This coefficient α can be either manually set up as a fixed value, or implemented by a scheduler
 1132 starting from 0 to some preset upper limit. The R_t in $L_\theta(h_{t,i}, a_{t,i})$ and $L_{\theta^c}(h_{t,i})$ is replaced by the
 1133 above $R_{t,i}$. To clarify this change, the two new losses are expressed as: $\hat{L}_\theta(h_{t,i}, a_{t,i})$ and $\hat{L}_{\theta^c}(h_{t,i})$.

1134 Furthermore, it is needed to search the underlying factorization scheme of the transition function in
 1135 the Dec-POMDP, according to Theorem 4.7. To implement this requirement, we need to fulfil the
 1136 following condition:

$$1137 \quad \sum_{i=1}^M V_i(h_{t,i}) = V(\mathcal{M}, h_t). \quad (23)$$

1140 The above equality is implemented as a regularization term during training.

1141 To maintain consistency with the critic losses, we consider to use the λ -return denoted by \hat{G}_t^λ to
 1142 represent $V(\mathcal{M}, h_t)$. In turn, the above equation can be expressed as:

$$1144 \quad V(\mathcal{M}, h_t) = \mathbb{E}_\pi [G_t^\lambda | h_t],$$

1146 where each $\hat{G}_{t:t+n}$ contributing to the \hat{G}_t^λ represented in $\text{TTD}(\lambda)$ is expressed as follows:

$$1148 \quad \hat{G}_{t:t+n} = R_t + \gamma R_{t+1} + \cdots + \gamma^{n-1} R_{t+n-1} + \gamma^n V(\mathcal{M}, h_{t+n}) \\ 1149 \\ 1150 \quad = R_t + \gamma R_{t+1} + \cdots + \gamma^{n-1} R_{t+n-1} + \gamma^n \sum_{i=1}^M V_i(h_{t+n,i}) \quad (\text{By Eq. 23}).$$

1153 Substituting the above formula into Eq. 23, we can obtain the regularization term referred to as the
 1154 **efficiency loss** for one timestep t , as follows:

$$1155 \quad L_{\theta^c}^e(h_{t,i}) = \frac{1}{2} \left(\hat{G}_t^\lambda - \sum_{i=1}^M V_i^{\theta^c}(h_{t,i}) \right)^2.$$

1159 In summary, the total loss function of Shapley Machine for POAM (SM-POAM) is as follows:

$$1161 \quad L_{\text{SM-POAM}} = \frac{1}{T} \sum_{t=1}^T \left(\sum_{i \in \mathcal{C}_t} \hat{L}_\theta(h_{t,i}, a_{t,i}) + \beta_1 \sum_{i \in \mathcal{M}} \hat{L}_{\theta^c}(h_{t,i}) + \beta_2 L_{\theta^c}^e(h_{t,i}) + L_{\theta^e, \theta^o, \theta^a}(h_{t,i}, o_{t,-i}, a_{t,-i}) \right),$$

1164 where T is the episode length; $\beta_1, \beta_2 \in (0, 1)$ are two coefficients to control the importance of the
 1165 two losses; as well as \mathcal{C}_t indicates the controlled agent set at timestep t and \mathcal{M} indicates the ad hoc
 1166 team following the convention in Wang et al. (2025).

1167 Similarly, the total loss function of Shapley Machine for IPPO (SM-IPPO) is as follows:

$$1169 \quad L_{\text{SM-IPPO}} = \frac{1}{T} \sum_{t=1}^T \left(\sum_{i \in \mathcal{C}_t} \hat{L}_\theta(h_{t,i}, a_{t,i}) + \beta_1 \sum_{i \in \mathcal{M}} \hat{L}_{\theta^c}(h_{t,i}) + \beta_2 L_{\theta^c}^e(h_{t,i}) \right).$$

1172 **Implementation of $k'_C > 0$.** As mentioned in Section 4.1, it is necessary to fulfil $k'_C > 0$ for
 1173 reaching cooperation, which can be implemented following the convention of $\text{TD}(\lambda)$ in RL (Sutton,
 1174 1988). Specifically, the weightings for m basis games $(k'_{C_1}, k'_{C_2}, \dots, k'_{C_m})$ are generated using a
 1175 geometric distribution P_λ with the parameter $0 < \lambda < 1$, such that $k'_{C_n} = P_\lambda(n)$, resulting a tuple
 1176 $((1 - \lambda), (1 - \lambda)\lambda, \dots, (1 - \lambda)\lambda^{m-1}, \lambda^m)$. With this condition, Eq. 8 becomes the TD error of the
 1177 well-known **truncated $\text{TD}(\lambda)$ prediction**, shortened as **TTD(λ)** (Cichosz, 1994).

1179 **Partial Observations.** In practice, a controlled agent is only able to receive an observation, following
 1180 the settings of Dec-POMDPs. Therefore, an agent is required to infer the state of the environment as
 1181 an individual hidden state, through the history of observations. To this end, the policy and individual
 1182 networks are realized by recurrent neural networks (RNNs) (e.g., GRUs (Chung et al., 2014)), where
 1183 observations or representations transformed from observations are as inputs. In implementation,
 1184 we use two base algorithms satisfying the conditions of partial observations: POAM (Wang et al.,
 1185 2025) and IPPO (De Witt et al., 2020) to realize Shapley Machine, referred to as: **SM-POAM** and
 1186 **SM-IPPO**, respectively.

1187 **Implementation of the Symmetry Axiom.** It can be observed that both POAM and IPPO are
 1188 implemented by the sharing parameters, with agent ID to differentiate agent identities. Given an agent

1188 ID, its input is either individual observations or individual observations + teammate embeddings,
 1189 where the teammate embeddings are transformed from individual observations. As per Remark 4.9,
 1190 **the structures of SM-POAM and SM-IPPO satisfies the Symmetry axiom.**

1191 **Estimation of Uncontrolled Agent Individual Values.** We maintain all possible controlled agent
 1192 policy and individual values networks as implemented by Wang et al. (2025), given that the maximum
 1193 number of controlled agents is known in the experimental settings of the NAHT, but only part of
 1194 controlled agents in an episode can make decision. Thanks to the sharing parameters technique, this
 1195 can be simply implemented by maintaining one policy or individual value network with a tuple of
 1196 agent IDs across all possible controlled agents. During the training phase, the uncontrolled agent
 1197 individual values are also required to implement the Efficiency axiom, as informed in Eq. 11, but
 1198 they are unknown to controlled agents. To this end, the uncontrolled agent individual values are
 1199 approximated by the maintained individual values of the controlled agents which are not activated.

1200 E.1.2 POAM AND IPPO

1201 The implementations of POAM and IPPO have been detailed in Appendix B.3.

1202 In summary, the total loss function of POAM is as follows:

$$1206 L_{\text{POAM}} = \frac{1}{T} \sum_{t=1}^T \left(\sum_{i \in \mathcal{C}_t} L_{\theta}(h_{t,i}, a_{t,i}) + \beta_1 \sum_{i \in \mathcal{M}} L_{\theta^c}(h_{t,i}) + L_{\theta^e, \theta^o, \theta^a}(h_{t,i}, o_{t,-i}, a_{t,-i}) \right).$$

1209 The total loss function of IPPO is as follows:

$$1211 L_{\text{IPPO}} = \frac{1}{T} \sum_{t=1}^T \left(\sum_{i \in \mathcal{C}_t} L_{\theta}(h_{t,i}, a_{t,i}) + \beta_1 \sum_{i \in \mathcal{M}} L_{\theta^c}(h_{t,i}) \right).$$

1214 E.1.3 BANZHAF MACHINE

1216 The overall loss function and implementation of the Banzhaf Machine closely follow those of POAM
 1217 and IPPO. The only distinction is that Banzhaf Machine employs TTD(λ) in place of the TD(λ) used
 1218 in POAM and IPPO.

1220 E.2 EXPERIMENTAL DOMAINS

1221 We now briefly introduce the experimental domains for running experiments. If one would like to
 1222 know more about details, please refer to Wang et al. (2025).

1224 E.2.1 MPE PREDATOR PREY (MPE-PP)

1226 The MPE Predator Prey (MPE-PP) environment is a predator-prey task implemented within the Multi-
 1227 Agent Particle Environment (MPE) framework. It simulates interactions within a two-dimensional
 1228 space populated by two static obstacles, where three pursuer agents must cooperate to capture a
 1229 single adversarial evader. A successful capture is defined as at least two pursuers simultaneously
 1230 colliding with the evader, upon which the pursuers receive a positive reward of +1. If the capture
 1231 is unsuccessful, no reward is granted. This environment is designed to test the ability of agents to
 1232 coordinate under spatial and dynamic constraints.

1234 E.2.2 THE STARCRAFT MULTI-AGENT CHALLENGE (SMAC)

1235 The StarCraft Multi-Agent Challenge (SMAC) serves as a benchmark suite for evaluating MARL
 1236 algorithms in partially observable, cooperative settings. Built atop the StarCraft II game engine,
 1237 SMAC presents a variety of micromanagement tasks where each agent (e.g., a Marine or Stalker)
 1238 operates based on limited local observations and must coordinate actions with teammates to overcome
 1239 enemy units. In this work, we focus on four specific SMAC scenarios: **5v6**: Five allied Marines
 1240 versus six enemy Marines, **8v9**: Eight allied Marines versus nine enemy Marines, **10v11**: Ten allied
 1241 Marines versus eleven enemy Marines, **3s5z**: Three allied Stalkers versus five enemy Zealots. At each
 timestep, agents receive a shaped reward proportional to the damage they inflict on opponents, along

1242 with bonus rewards of 10 points for each enemy defeated and 200 points for achieving overall victory
 1243 by eliminating all adversaries. The total return is normalized so that the maximum achievable return
 1244 in each scenario is 20. The action space in SMAC is discrete, enabling each agent to choose actions
 1245 such as attacking a particular enemy, moving in a specific direction, or remaining idle. Notably, the
 1246 variation in the number and type of agents and opponents across tasks results in scenario-specific
 1247 observation and action space dimensionalities, thereby introducing further diversity and complexity
 1248 for algorithmic evaluation. The length of an episode varies across different scenarios: MPE-PP with
 1249 $T = 100$, 3sv5z with $T = 250$, 5v6 with $T = 70$, 8v9 with $T = 120$ and 10v11 with $T = 150$.

1250 E.3 EVALUATION METRICS

1251 For in-distribution evaluation, the mean return (or winrate) is computed over E randomly sampled
 1252 episodes. In each episode, we form a joint policy $\pi^{(\mathcal{M})}$ by sampling N agents uniformly from \mathcal{C}
 1253 and the remaining $M - N$ agents from \mathcal{U} . For the out-of-distribution (OOD) evaluation, the M–N
 1254 score (Wang et al., 2025) is applied. Given a set of controllable agents \mathcal{C} and uncontrolled agents \mathcal{U} ,
 1255 the M–N score measures how well mixed teams of these agents cooperate in the NAHT setting. The
 1256 score is computed exhaustively by varying the number of controllable agents included in the team.
 1257 Specifically, for each $N \in \{1, \dots, M - 1\}$, we form a joint policy $\pi^{(\mathcal{M})}$ by sampling N agents
 1258 uniformly from \mathcal{C} and the remaining $M - N$ agents from \mathcal{U} . The mixed team is then evaluated on the
 1259 task for E episodes. This procedure yields $(M - 1) \cdot E$ returns (or winrates) in total, whose average
 1260 defines the M–N score. For the OOD evaluation on unseen conventions, the M–N score is computed
 1261 by averaging the per-convention M–N scores across 4 other conventions for each agent type. For the
 1262 OOD evaluation on unseen agent types, the per-convention M–N score is computed by averaging
 1263 the per-convention M–N score across 5 conventions for each unseen agent type. Each convention of
 1264 uncontrolled agents is a random seed that pretrains them. All results are obtained by first computing
 1265 each metric with 128 episodes and then averaging these per-seed metrics across 5 random seeds, with
 1266 95% confidence intervals reported.

1267 E.4 EXPERIMENTAL SETTINGS

1268 The training procedure of the n-agent ad hoc teamwork (NAHT) process is briefly introduced here.
 1269 For more details, please refer to Wang et al. (2025). For each scenario (e.g. MPE, 3sv5z, 5v6,
 1270 8v9 and 10v11), there are five groups of pretrained agents (e.g. IQN, MAPPO, VDN, QMIX and
 1271 IPPO) acting as the uncontrolled agents. For each episode evaluation, the number of uncontrolled
 1272 agents $M - N$ is sampled, and then a group of pretrained agents is sampled. Given that each task
 1273 specifies a fixed total number of agents M , the number of controlled agents is N . **Note that this**
 1274 **is still a special case of openness. For a varying number of controlled agents, the number of**
 1275 **uncontrolled agents is also varied in correspondence, constrained by the total number of agents**
 1276 **related to the task specifications.** The distribution for all sampling procedures are modelled as the
 1277 multinational distribution with no replacement. Each uncontrolled agent executes the greedy policy
 1278 in both training and testing procedures. In contrast, each controlled agent executes the on-policy
 1279 sampling via the parameterized policy during the training procedure, while the greedy policy during
 1280 the testing procedure.

1281 E.5 HYPERPARAMETER SETTINGS

1282 Since our algorithm is established based on POAM and IPPO, most hyperparameter settings follow
 1283 that in Wang et al. (2025). First, the actors and critics are implemented in recurrent neural networks,
 1284 with full parameter sharing. Specifically, they are implemented by two fully connected layers followed
 1285 by a GRU layer and an output layer. Each layer has 64 dimensions with a ReLU activation function,
 1286 and layer normalization is applied. The encoder-decoder networks for inferring agent characteristics
 1287 are also implemented in parameter sharing. The encoder is implemented by a GRU layer, followed
 1288 by a fully connected layer with a ReLU activation function and an output layer. The decoder is
 1289 implemented by two fully connected layers with ReLU activation functions, followed by an output
 1290 layer. Adam Optimizer is used to train all models. The detailed hyperparameter for experiments is
 1291 shown in Tables 1 and 2. For the scenarios such as MPE, 3sv5z and 5v6, the values of m are set
 1292 as the number of non-empty coalitions. For the scenarios such as 8v9 and 10v11, the values of m
 1293 is simply set as the length of an episode (see Appendix E.1 for more details). Note that the term
 1294

1296 $\sum_{j \neq i} (V_j(s_t) - \gamma V_j(s_{t+1}))$ in shaped rewards is standardised to match the scales of standardised
 1297 rewards. To stabilize learning in large-scale scenarios, we add a value loss clip to Shapley Machine
 1298 and Banzhaf Machine for POAM on both 8v9 and 10v11, and for IPPO on 10v11 only.
 1299

1300 Table 1: Key hyperparameters of Shapley and Banzhaf Machine: λ indicates the parameter for the
 1301 weighting functions of TTD(λ), m indicates the number of basis games, α controls the importance
 1302 of the term $\sum_{j \neq i} (V_j(s_t) - \gamma V_j(s_{t+1}))$ in Eq. 22, β_1 controls the importance of the critic loss
 1303 $\sum_{i \in \mathcal{M}} \hat{L}_{\theta^c}(h_{t,i})$, and β_2 controls the importance of the efficiency loss $L_{\theta^c}^e(h_{t,i})$.
 1304

Algorithm	Task	λ	m	α	β_1	β_2
Shapley Machine	MPE-PP	0.85	7	0.01	0.5	0.01
	3v5z	0.85	7	0.01	0.5	0.01
	5v6	0.85	31	0.01	0.5	0.001
	8v9	0.95	120	0.01	0.5	0.001
	10v11	0.95	150	0.01	0.5	0.001
Banzhaf Machine	MPE-PP	0.85	7	N/A	0.5	N/A
	3v5z	0.85	7	N/A	0.5	N/A
	5v6	0.85	31	N/A	0.5	N/A
	8v9	0.95	120	N/A	0.5	N/A
	10v11	0.95	150	N/A	0.5	N/A

1316
 1317 Table 2: Common hyperparameters of RL settings for both IPPO and POAM.
 1318

Hyperparameter	Value
LR	0.0005
Epochs	5
Minibatches	1
Buffer size	256
Entropy coefficient	0.05
Clip	0.2
ED LR	0.0005
ED epochs	1
ED Minibatches	1
Optim_alpha (Adam)	0.99
Optim_eps (Adam)	0.00001
Use_obs_norm	True
Use_orthogonal_init	True
Use_adv_std	True
Standardise_rewards	True
num_parallel_envs	8

E.6 COMPUTATIONAL RESOURCES

1339 All experiments are conducted on Intel Xeon Gold 6230 CPUs and Nvidia V100-SXM2 GPUs. Each
 1340 experiment run on MPE takes approximately 7 hours, utilizing 20 CPU cores and 1 GPU. Each
 1341 experiment run on SMAC takes between 8 and 19 hours, utilizing 30 CPU cores and 1 GPU. All
 1342 experiments are trained with 20M timesteps. The post-training evaluation for each scenario takes
 1343 between 6 and 16 hours, utilizing 8 CPU cores and 1 GPU.

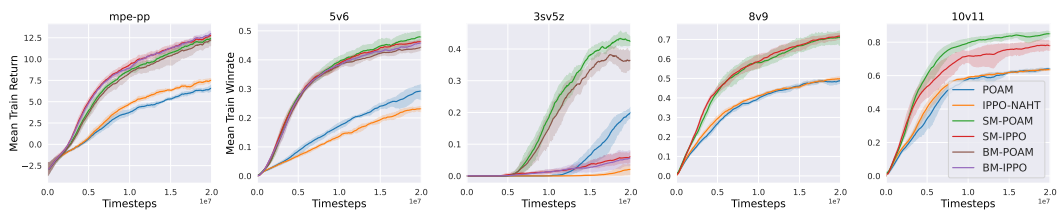
F ADDITIONAL EXPERIMENTS

F.1 EMPIRICAL EVIDENCE FOR THE STRENGTH OF THE AXIOMATIC FRAMEWORK

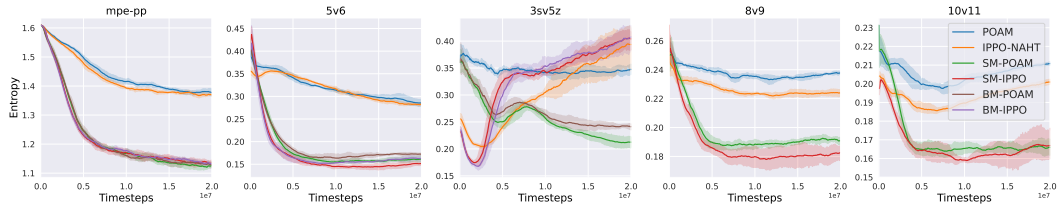
1344
 1345 We now discuss the phenomenon observed from the performance under stochastic policy
 1346 exploration during training. Discussing this phenomenon is meaningful. When a machine learning
 1347

1350 algorithm is deployed and has to adapt to real-world environments through online learning due to the
 1351 mismatch between simulators and real-world environments, it is expected that random exploration
 1352 diminishes rapidly over time to avoid the damage on real-world environments (e.g. physical systems).
 1353

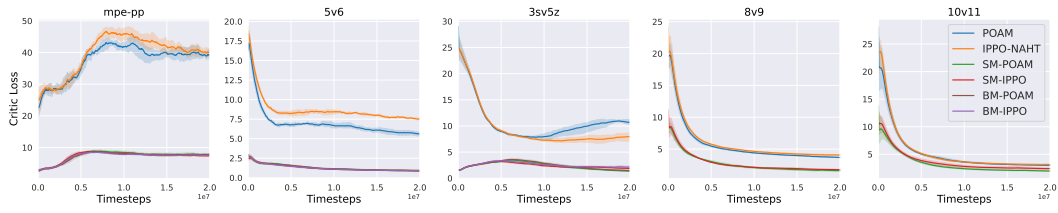
1354 Recall that the PPO family algorithms implement exploration by the natural stochastic policy sampling
 1355 from the learned policy distribution and maximizing policy entropy. As seen from Figure 7, either
 1356 Shapley- or Banzhaf-based algorithms can outperform their base algorithm counterparts with a large
 1357 margin. The reasons are as follows. As shown in Figure 8, policy entropy decreases rapidly over
 1358 the course of training (except for the IPPO implementation on 3sv5z, which underperforms due
 1359 to incompatibility between IPPO and the task). This indicates that the learned policies become
 1360 more deterministic than those of the base algorithms, despite all methods being optimized with
 1361 an entropy-maximization objective. A possible explanation for this phenomenon is illustrated in
 1362 Figure 9: the critic loss of Shapley and Banzhaf Machine decreases faster than that of their base
 1363 algorithm counterparts. **This provides evidence for the advantage of structured individual value
 1364 functions under our proposed axiomatic framework.**



1364
 1365 Figure 7: Performance under the stochastic exploration policy during training in NAHT.
 1366
 1367
 1368
 1369



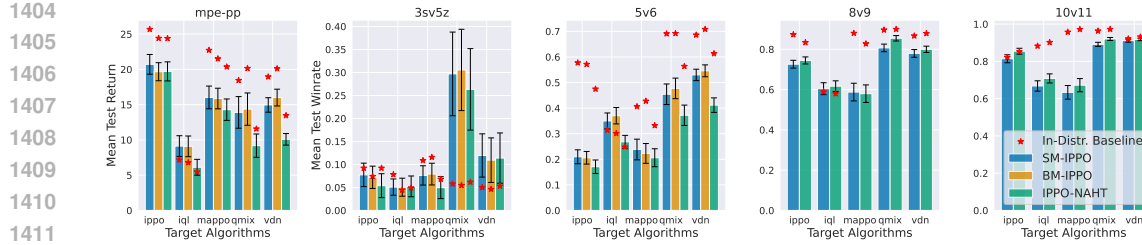
1370
 1371 Figure 8: Policy entropy across scenarios during training in NAHT.
 1372
 1373



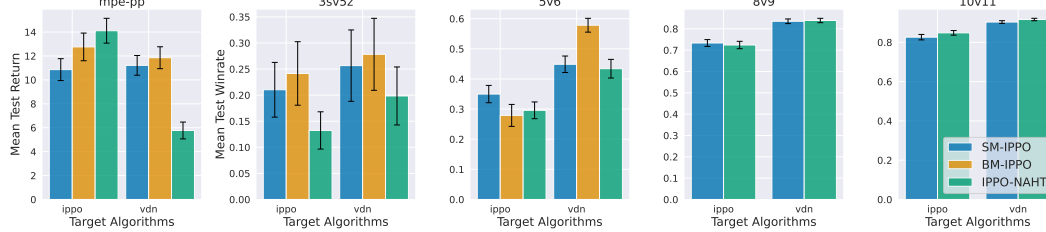
1374
 1375 Figure 9: Critic loss across scenarios during training in NAHT.
 1376
 1377
 1378
 1379
 1380

1381 F.2 ANALYZING EFFECTS OF EFFICIENCY AXIOMS 1382

1383 We now demonstrate the association between the changing of the mean shaping rewards and the
 1384 response of corresponding testing returns. As shown in Figure 12, the shaped rewards increases
 1385 in the beginning and then gradually reaches a plateau. The efficiency loss also exhibits the similar
 1386 phenomenon. As shown in Figure 13, it can be observed that when instability happens during training
 1387 as evidenced by the sudden changes of test returns, the shaped rewards can consistently manifest
 1388 this situation (as highlighted in red vertical dashed lines). This feature is crucial in the NAHT, since
 1389 it could be a frequent and typical case when an unseen agent appears in the environment, which
 1390 may perturb the training stability. **This justifies the effectiveness of the shaping rewards $R_{t,i}$ we
 1391 propose to fulfil the Efficiency axiom. More importantly, this highlights the importance and
 1392 necessity of the Efficiency axiom to perceive and measure the changing of environments.**



(a) Evaluation on unseen conventions (identical algorithms with different random seeds). The star denotes the in-convention baseline, and the histograms show performance on unseen conventions with error bars.



(b) Evaluation on unseen agent types. Train set: MAPPO, QMIX, IQL; test set: IPPO, VDN.

Figure 10: Out-of-distribution (OOD) evaluation after training, assessing unseen conventions and unseen agent types during training, between learned agents (IPPO-NAHT, SM-IPPO and BM-IPPO) and uncontrolled agent types (IPPO, VDN, IQL, QMIX and MAPPO). The performance is evaluated by averaging all pairings of N controlled and $M - N$ uncontrolled agents and their corresponding random seeds, called M–N score (Wang et al., 2025).

F.3 EXTRA RESULTS OF OOD EVALUATION

We also conducted experiments on evaluating the OOD performance of Shapley Machine and Banzhaf Machine on the base algorithm IPPO (IPPO-NAHT). As seen from Figure 10a, Banzhaf Machine is competitive to Shapley Machine on dealing with unseen conventions. Although it seems the result is opposite to the conclusion drawn from the POAM related results, the underlying reason could be the general weaker performance of IPPO than POAM due to the lack of agent modelling, as shown in Figure 14. This could inhibit the full capability of Shapley Machine. As seen from Figure 10b, the general performance of Banzhaf Machine is better than Shapley Machine. This is consistent with the conclusion drawn from the POAM related results. In Figure 11, we show additional comparisons between algorithms: POAM vs. IPPO, SM-POAM vs. SM-IPPO and BM-POAM vs. BM-IPPO. **We find no strong evidence that the axioms are sensitive to the choice of base algorithm.**

F.4 POTENTIAL INSTABILITY OF SHAPLEY MACHINE FOR LARGE-SCALE SCENARIOS

During our repeated trials, we observe that the performance of Shapley Machine is not stable in large-scale scenarios (e.g. 8v9 and 10v11), compared with in small-scale scenarios (e.g. MPE-PP, 3sv5z and 5v6). We now analyze the potential reason behind this phenomenon. As observed from Figures 15 and 16, it can be confirmed that **the instability of shaped rewards is the key reason to cause the instability of learning procedure for large-scale scenarios**. According to the functionality of shaping rewards discussed in Appendix F.2, we hypothesize that **the instability could be caused by the unstable changing of value difference in the shaping reward: $\sum_{j \neq i} (V_j(s_t) - \gamma V_j(s_{t+1}))$** . Specifically, when the number of agents increases, the accumulating prediction error of individual value functions will be amplified.

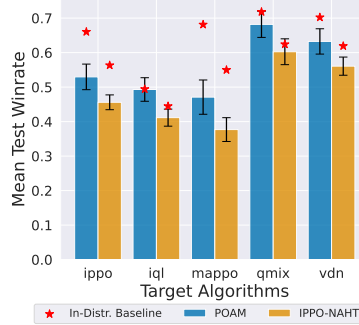
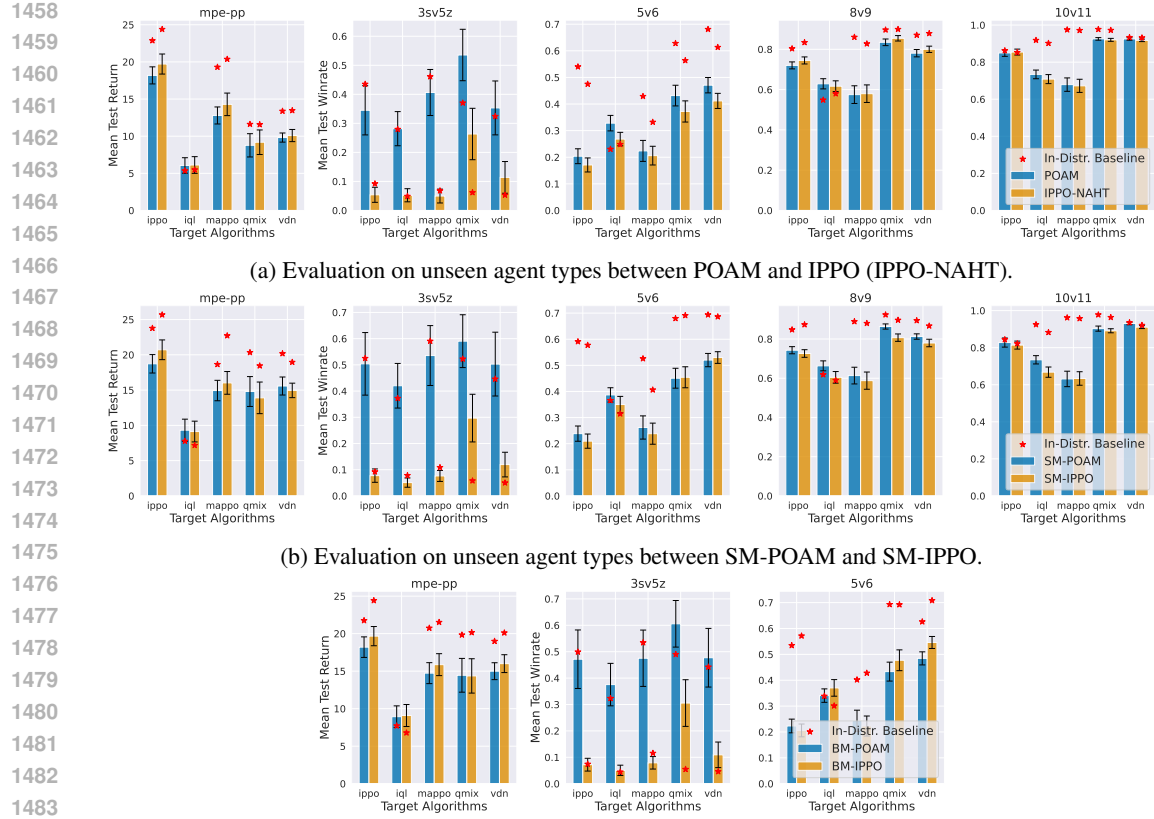
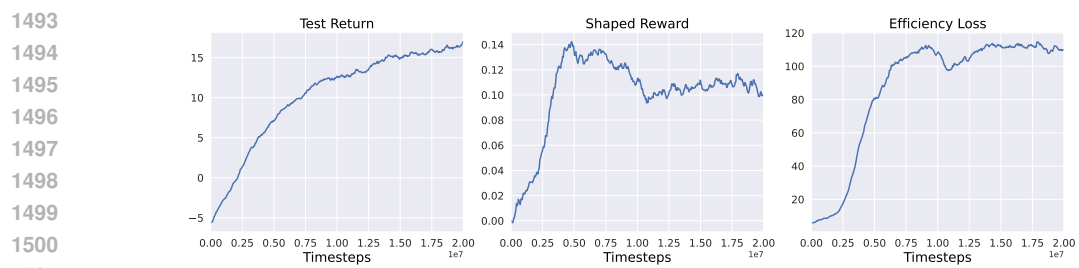


Figure 14: Average evaluation performance on unseen conventions across 4 SMAC tasks. The star denotes the in-convention baseline, and the histograms denotes the unseen conventions.



1463 (c) Evaluation on unseen agent types between BM-POAM and BM-IPPO. Since the implementation of Banzhaf
1464 Machine is equivalent to its counterpart baseline algorithms for 8v9 and 10v11 due to approximating the number
1465 of non-empty basis games as the episode length, we ignore their evaluation here.

1466 Figure 11: Out-of-distribution (OOD) evaluation after training, assessing unseen conventions during
1467 training, between learned agents (IPPO-NAHT, SM-IPPO, and BM-IPPO) and uncontrolled agent
1468 types (IPPO, VDN, IQL, QMIX and MAPPO). The performance is evaluated by averaging all pairings
1469 of N controlled and $M - N$ uncontrolled agents and their corresponding random seeds, called M–N
1470 score (Wang et al., 2025).



1472 Figure 12: One run of MPE to show the variation of test return, shaped reward and efficiency loss.

1473 To mitigate the above issue, we have added the value loss clip to stabilize the learning procedure
1474 of individual value functions for the large-scale scenarios such as 8v9 and 10v11. As seen from
1475 Figure 3, even with the value loss clip the instability of SM-IPPO is still out of control. This could be
1476 the cascading effect caused by the lack of agent modelling in contrast to SM-POAM, the instability
1477 of which is far beyond the capability of value loss clip. On the other hand, this reflects **the value of
1478 agent modelling in POAM for tackling the large-scale multi-agent scenarios**.

1479 As seen from Figure 17, the learning procedures with the value loss clip for the SM-POAM apparently
1480 perform more stably than those without. This verifies our initial hypothesis. Due to this strategy will



Figure 13: One run of 5v6 to show the variation of test return, shaped reward and efficiency loss.

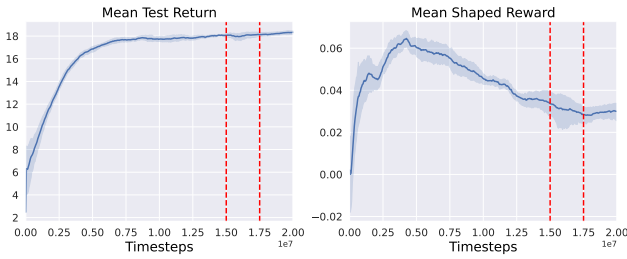


Figure 15: A case of 8v9 with SM-POAM to show the instability of learning progress via the mean shaped rewards. The range bounded by two red dashed lines shows the fluctuation of the learning process.

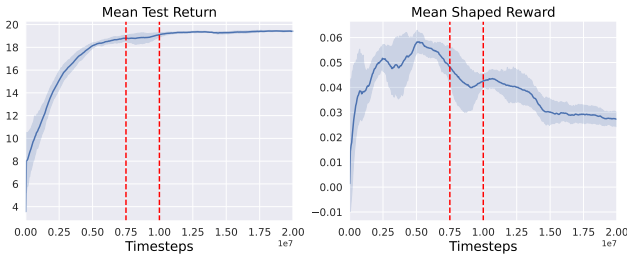


Figure 16: A case of 10v11 with SM-POAM to show the instability of learning progress via the mean shaped rewards. The range bounded by two red dashed lines shows the fluctuation of the learning procedure.

slow down and even hinder the performance for the other three scenarios, we have not posted this as a common strategy. **We believe this deserves further investigation in the future before any claims can be made about its general performance.**

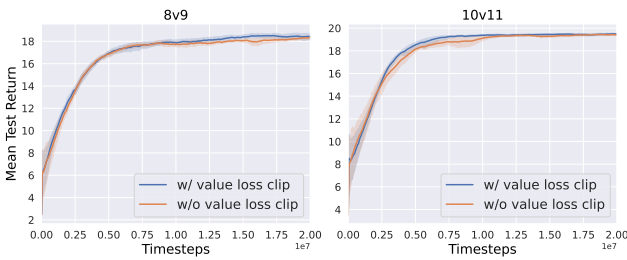


Figure 17: Comparison between the learning procedure of SM-POAM with and without the value loss clip in the 8v9 and 10v11 scenarios.

1566
1567

F.5 OOD EVALUATION ACROSS DIFFERENT NUMBERS OF CONTROLLED AGENTS

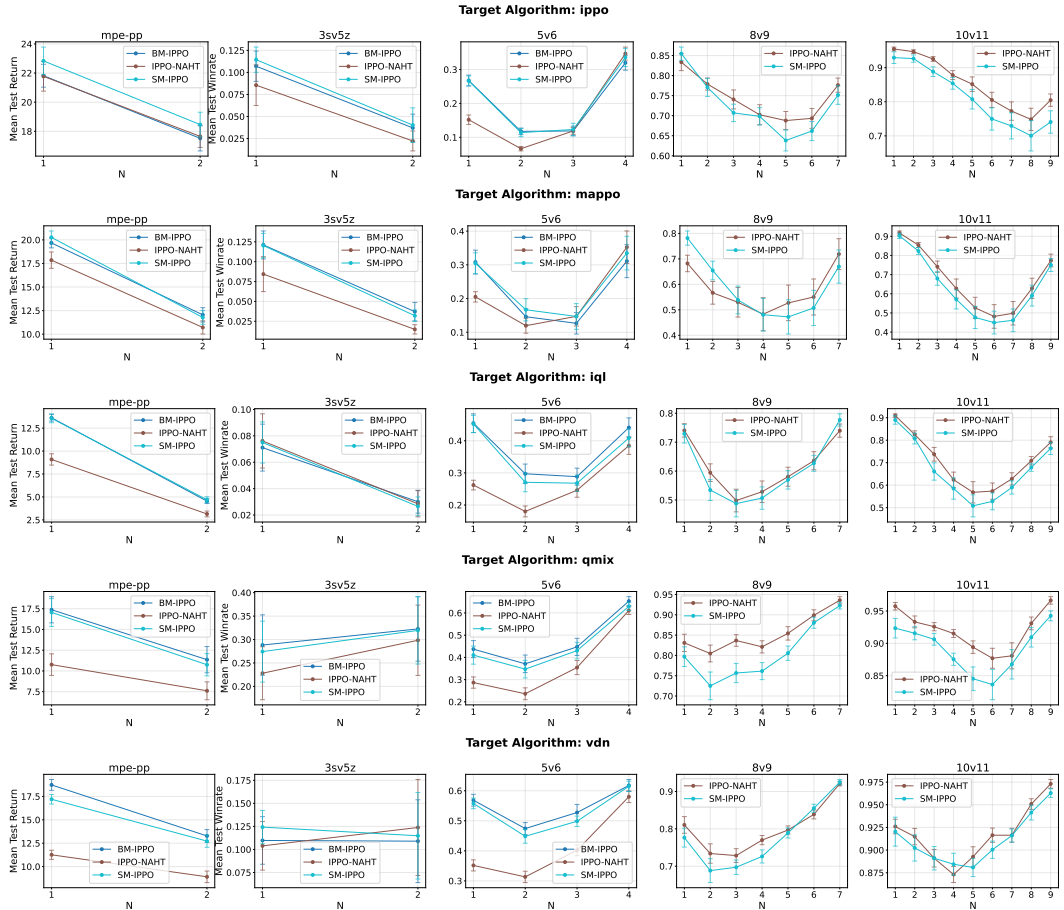
1568
1569
1570
1571
1572
1573
1574
1575
1576We report the results on unseen conventions and agent types across each specific number of controlled agents N in Figures 18–21, by fixing the N value in the M–N score.1577
1578
1579
1580
1581
1582
1583
1584
1585
1586
1587
1588
1589
1590
1591
1592
1593
1594
1595
1596
1597
1598
1599
1600
1601
1602
1603
1604
1605
1606
1607
1608
1609
1610
1611
1612
1613
1614
1615
1616
1617
1618
1619

Figure 18: Out-of-distribution (OOD) evaluation after training, assessing unseen conventions during training, between learned agents (IPPO-NAHT, SM-IPPO and BM-IPPO) and uncontrolled agent types (IPPO, VDN, IQL, QMIX and MAPPO).

Target Algorithm: ippo

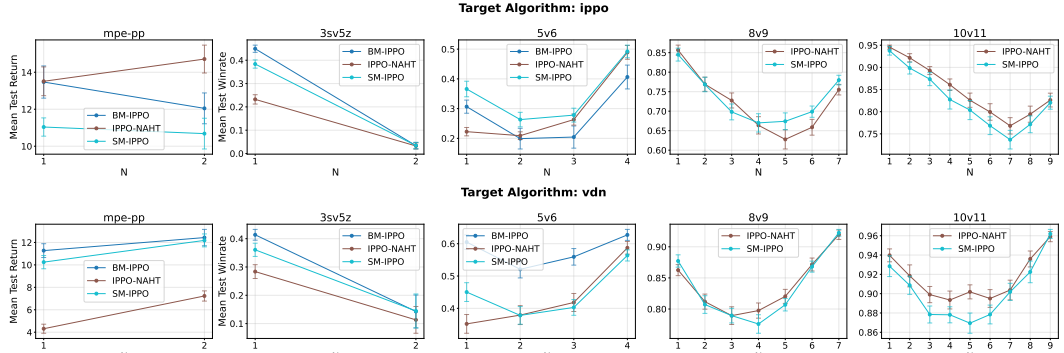


Figure 19: Out-of-distribution (OOD) evaluation after training, assessing unseen agent types during training, between learned agents (IPPO-NAHT, SM-IPPO and BM-IPPO) and unseen uncontrolled agent types (IPPO and VDN).

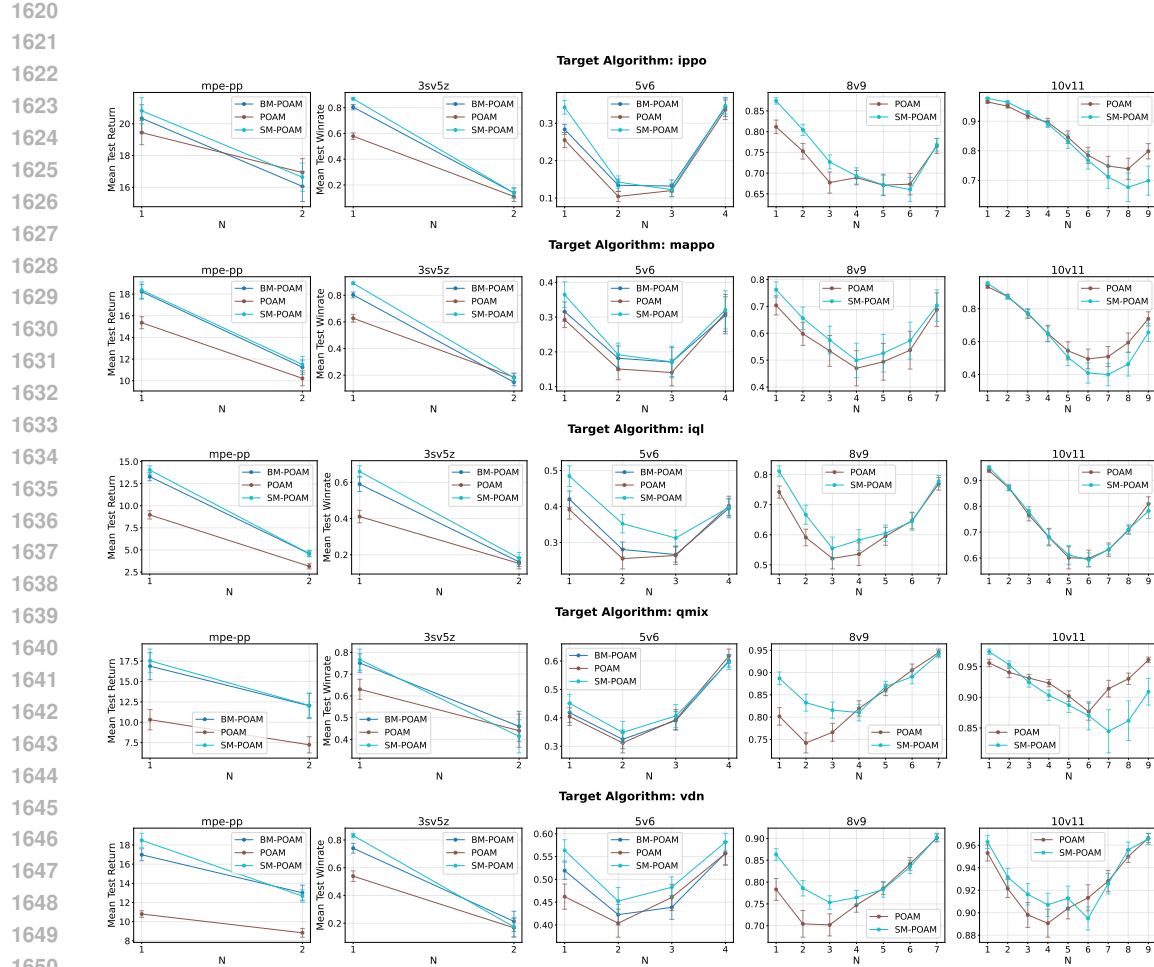


Figure 20: Out-of-distribution (OOD) evaluation after training, assessing unseen conventions during training, between learned agents (POAM, SM-POAM, and BM-POAM) and uncontrolled agent types (IPPO, VDN, IQL, QMIX and MAPPO).

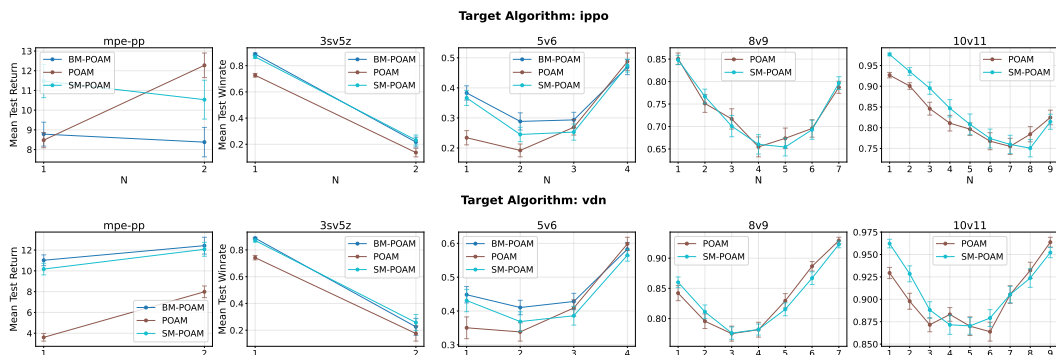


Figure 21: Out-of-distribution (OOD) evaluation after training, assessing unseen agent types during training, between learned agents (POAM, SM-POAM and BM-POAM) and unseen uncontrolled agent types (IPPO and VDN).